

Chemical Sensing Applications of Fiber Optics

by

Anjana Nagarajan

Thesis submitted to the Faculty of the
Virginia Polytechnic Institute and State University
in partial fulfillment of the requirements for the degree of
MASTER OF SCIENCE

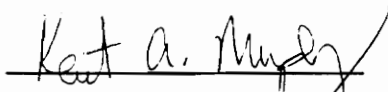
in

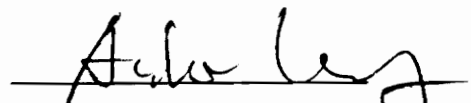
Electrical Engineering

APPROVED:



Dr. Richard O. Claus, Chairman


Dr. Kent A. Murphy


Dr. Anbo Wang

May 1994
Blacksburg, Virginia

LD
5655
V855
1994
N343
C.2

Chemical Sensing Applications of Fiber Optics

by

Anjana Nagarajan

Richard O. Claus, Chairman

Bradley Department of Electrical Engineering,
Virginia Polytechnic Institute and State University

(ABSTRACT)

A sensing method that can monitor metallic structures continuously would eventually produce safer metallic structures as well as a more efficient and economic way to monitor corrosion. A secondary focus of this research is the implementation of a fiber optic sensor to measure refractive indices of unknown solutions.

The surface plasmon sensor, interrogated with white light resulted in attenuations of light at different wavelengths when solutions of different refractive indices were introduced. This sensor has been shown to respond to the three configurations of polished single mode and multimode, as well as the unpolished multimode sensors. The sensitivity calculated was comparable with the sensitivity of the Kretschmann arrangement.

The transmissive aluminum-clad fiber sensor was shown to be effective in providing a response to the process of corrosion. Varying lengths of aluminum-clad fiber was spliced to acrylate multimode fiber and different wavelengths of sources were used to test the sensor in a bath of NaOH. The results were similar and reproducible. A tapered sensor configuration was attempted and proved to be very useful.

ACKNOWLEDGMENTS

I would like to thank Dr. Claus for his guidance, motivation and support. I also thank him for giving me the opportunity to work at FEORC. I would like to thank Dr. Murphy for his continuous encouragement and always making my work seem a little easier. I also thank Dr. Wang for his help and guidance in the past two years.

I thank Ron Earp for his help with the surface plasmon experiments and having the patience to wait till we saw the first surface plasmon move. I would also like to thank Vivek Arya for his assistance. I am grateful to Mark Miller for all his guidance and help with the aluminum-clad fiber project.

I thank all the members of FEORC, who have made the last few years an exciting learning experience, especially Asif, Dave, Nirmal, Rajat, Sridhar, Veeru and many others for their friendship and assistance.

I am grateful to my roommates and friends; Asela, Mallika, Pablo and Sammy for putting up with me and being so supportive this year.

I thank Vikas for being my friend and making life more fun and challenging. I am very grateful for all his support and encouragement.

Last but not the least, I am eternally grateful to my family; my father S. Nagarajan, my mother, Alamelu and my brother Anand for their love and support. I definitely would not have been able to make it this far without them.

TABLE OF CONTENTS

TABLE OF CONTENTS	iii
1.0 INTRODUCTION.....	1
1.1 Definition of an optical fiber	1
1.2 Definition of a fiber optic sensor	1
1.3 Advantages of optical fiber sensors.....	2
1.4 Types of fiber optic sensors	2
2.0 HISTORICAL	7
2.1 Corrosion detection techniques.....	7
2.2 Aluminum-clad transmissive sensor	10
2.3 Kretschmann Surface Plasmon Resonance Device.....	11
2.4 Applications of Prism-Based SPR Devices:.....	13
2.5 Fiber Optic SPR Devices	14
3.0 THEORY	17
3.1 Theory of Prism-Based SPR Devices	17
3.2 Theory of Fiber-Based SPR Devices.....	19
3.2.1 The Three Layer SPR System	20
3.2.2 The Four Layer SPR System.....	29
3.3 The Transmissive Aluminum-Clad Fiber Corrosion Sensor System	34
4.0 SENSOR CONSTRUCTION	39
4.1 Three Layer Surface Plasmon Sensor.....	39
4.2 Transmissive Aluminum-Clad Fiber Sensor	42
5.0 EXPERIMENTAL SETUP.....	46
5.1 Experimental setup of the prism SPR sensors.....	46
5.2 Experimental Setup of Fiber SPR Sensors	49

5.3 Aluminum-Clad Transmissive Sensor.....	50
6.0. EXPERIMENTAL RESULTS AND DISCUSSION.....	53
6.1 Experimental Results and Discussion of the Kretschmann Prism Experiment.....	53
6.2 Experimental Results and Discussion of the Three Layer SPR Experiments	53
6.1.1 The single mode fiber sensors.....	55
6.2.2 Polished multimode fiber sensors.....	55
6.2.3 Multimode unpolished fiber sensors	58
6.3 Applications of the fiber-based surface plasmon sensor	63
6.4 Future Work with the Fiber-based SPR Sensors.....	64
6.5 Aluminum-clad fiber sensor experimental results and discussion.....	64
6.6 Applications of the aluminum-clad fiber sensor	69
6.7 Future Work with aluminum-clad fiber sensors	69
7.0 CONCLUSIONS	72
REFERENCES.....	74

LIST OF FIGURES

1.1 A typical electrical field versus its phase	4
1.2 The corresponding intensity of the electrical field versus the phase	4
2.1 The Kretschmann prism configuration	12
2.2 The setup for fiber based SPR sensors	16
3.1 Wavevector matching	19
3.2 The three layer fiber SPR configuration	22
3.3 Dispersion plot of Bender equation	25
3.4 Experimental results of the Bender 3-layer SPR test	26
3.5 Dispersion plot of the Johnstone equation	27
3.6 Theoretical response of 3-layer SPR sensor with a silver overlay	28
3.7 Theoretical response of 3-layer SPR sensor with aluminum overlay	29
3.8 The four layer SPR configuration	31
3.9 Dispersion equation of the Bender-Miller equation	33
3.10 Results of the four layer experiment	34
3.11 The setup of the cutback test.....	37
4.1 Schematic of the polishing setup for 3-layer SPR sensors	42
4.2 Wavelength vs. refractive index dependenc of the 3-layer configuration.....	43
4.3 The splice of the aluminnum-clad and multimode fiber.....	47
5.1 The setup for prism based sensors	50
5.2 The setup for fiber based SPR sensors	52
5.3 The setup of the NaOH etch test with the aluminum-clad fiber sensor.....	54
6.1 SPR test on Kretschmann prism arrangement	57

6.2 Sample waveform of a SM polished fiber SPR sensor, sample RI = 1.4142.....59

6.3 Wavelength of observed SPR with sample RIs using the SM polished sensor..... 60

6.4 (a) Sample waveform of a MM polished fiber SPR sensor, sample RI = 1.333 61

6.4 (b) Sample waveform of a MM polished fiber SPR sensor, sample RI = 1.4172 61

6.5 Wavelength of observed SPR with sample RIs using the MM polished sensor..... 63

6.6 (a) Sample waveform of a MM unpolished SPR sensor, sample RI = 1.3595 64

6.6 (b) Sample waveform of a MM unpolished SPR sensor, sample RI = 1.3856 64

6.7 Wavelength of observed SPR with sample RIs using MM unpolished sensor..... 65

6.8 Output power vs. time for an aluminum-cald fiber test using a 1300 nm source..... 68

6.9 Output power vs. time for an aluminum-cald fiber test using a 850 nm source 69

6.10 Output power vs. time for an aluminum-cald fiber test using a 633 nm source..... 70

6.11 Comparison of the output power vs. time for a normal and 4-level tapered
 sensor 74

1.0 INTRODUCTION

1.1 Definition of an optical fiber

An optical fiber consists of a core with a high refractive index as compared to the refractive index of the glass cladding that surrounds it. The lower refractive index of the cladding causes light incident on the fiber to be totally internally reflected at the core/cladding interface. The cladding reduces scattering losses resulting from dielectric discontinuities at the core surface and provides mechanical support to the fiber. The cladding is surrounded by a mechanical jacket of polymeric or metallic origin to provide further mechanical and moisture protection and mechanically isolate the fibers from small geometrical irregularities or distortions of adjacent surfaces.

1.2 Definition of a fiber optic sensor

A sensor is a device that converts the state of a physical measurand into a easily readable form. Sensors are present and very widely used in all walks of life. A smoke alarm in a kitchen, a thermometer that reads temperature, or a guidance detector in a rocket are all sensors. A sensor that is constructed based upon the physical properties of the optical fiber can be generally referred to as a fiber optic sensor. Over the past fifteen years, the use of optical fibers as sensors has been widely implemented for applications in the characterization of aerospace and hydrospace materials and structures, civil structures, industrial process and control, biomedical and biochemical systems.¹ The rapid progress of optical telecommunications technology in the same time frame has helped commercialize fiber-optic based smart structures.

1.3 Advantages of optical fiber sensors

Optical fiber sensors exhibit many unique features that corresponding electronic and mechanical sensors cannot match:

- (1) High sensitivity and excellent resolution. Changes of optical phase can be detected very precisely.
- (2) Light weight and small size. Dielectric materials weigh much less than metals, a crucial advantage for aerospace applications and other precise sensitive applications.
- (3) Environmental ruggedness. Optical fibers are inherently immune to electromagnetic interference and may be ruggedized for vibration and shock. They also avoid ground loops.
- (4) High temperature performance. Optical fibers can be used to sense temperature and other physical parameters such as strain and pressure in a high temperature environment. Silica waveguides can withstand temperatures up to 900°C, sufficient for most airfoil surfaces; while sapphire waveguides can operate up to temperatures of 1900°C, making them ideal for engine environment.²

1.4 Types of fiber optic sensors

Optical fibers have been used to measure many environmental parameters such as temperature, strain, pressure, magnetic fields, corrosion, displacement, vibration, impact detection and acoustic waves.³⁻⁶ It has been demonstrated that fiber optic sensors can be classified into two general classes, intensity-modulated and phase-modulated sensors.

To better understand these concepts, let us express the electrical field inside an optical fiber in this simplified form,

$$E = A \sin (kx - \omega t + \Psi), \quad (1.1)$$

where A is the amplitude, k is the wave number, ω is the angular frequency and Ψ is the initial phase of the electric field. These four parameters are constants for a given field and a plot of the electric field versus the phase as shown in Figure 1.1. The intensity of this wave is defined as

$$I = \langle E^2 \rangle = A^2/2, \quad (1.2)$$

The operation of an intensity-modulated optical fiber sensor is based upon the fact that optical intensity varies due to changing environments such as temperature, displacement, speed of rotation and other factors. Most applications use wide band light sources such as LEDs and white light sources since they are more economical and easier to implement. Multimode fibers are ideal for intensity-modulated sensors and geometric optics are often applied to describe intensity-based sensor behavior. Intensity-based sensors use simple signal processing because only the amplitude of the received signal is important. The sensors of concern here are intensity-modulated sensors.

Phase-modulated or interferometric sensors operate based upon the change of phase term, $kx - \omega t + \psi$, due to changing environment. Mach Zehnder, Michelson, Sagnac and Fabry Perot fiber interferometers are examples of phase-modulated sensors.

The objective of this research is to perform chemical sensing using fiber optics for all the above mentioned reasons. One of the major objectives is to focus upon monitoring metallic corrosion. Corrosion is a serious problem in all metallic structures. A sensing system that can monitor metallic structures continuously for corrosion is more cost-effective than the conventional methods in which the corroding metallic structure is dismantled periodically and checked for corrosion. Applications can be found in the aircraft, spacecraft, ground transportation, energy production and distribution industries.

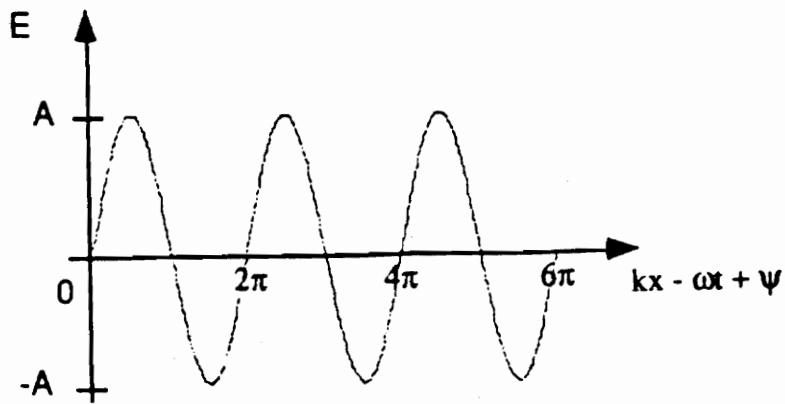


Figure 1.1 A typical electrical field versus its phase.

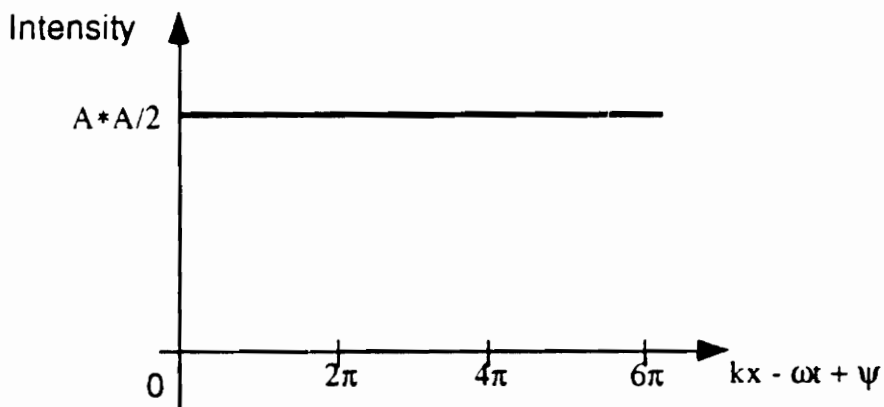


Figure 1.2 The corresponding intensity of the electrical field versus the phase.

Such a method of continuous monitoring would eventually produce safer metallic structures as well as a more efficient and economic way to monitor corrosion. The corrosion of aluminum was chosen as the primary focus of this research. A secondary focus is the implementation of a fiber optics sensor to measure refractive indices of solutions.

The sensor system described here is based on two concepts. The first is a type of intrinsic fiber sensor which functions by coupling optical energy propagating in the fiber to a surface plasmon on a metallic film which has been deposited onto the surface of the fiber.⁷ A small length of the lateral surface of the fiber is polished to within a micron of the core. Several thin films are applied to the polished section of the fiber. When a suitable chemical sample of a particular refractive index is brought into contact with the modified section of the fiber, energy in the fiber is resonantly coupled from the fiber core into an optical mode in the metal film. This metallic mode is the surface plasmon and the phenomenon is surface plasmon resonance. The resonance condition is monitored by an attenuation of light reaching the end of the fiber.

The coupling of energy between the core and plasmon is very strongly dependent on the refractive index of the chemical sample, which translates to an attenuation at a certain wavelength of light.⁷ The sensors tested here were injected with a white light source which caused attenuations at different wavelengins, as seen on the white light spectroscope. The interrogation of the sensor with white light produces a very broad sensor that is capable of sensing a wide variety of refractive indices. This sensor is very useful in sensing biomolecular interactions, specifically with regards to the measurement of

antibody-antigen constants. Also, by using aluminum as the metal layer, a response can be predicted that will sense the process of corrosion.

The second type of sensor is a transmissive aluminum-clad fiber sensor where the core of a standard fiber is coated with 40 micrometers of aluminum. Varying lengths of aluminum-clad fiber are mechanically spliced to standard multimode fiber of 140/180 micrometers core and cladding diameter respectively. Aluminum has a very high complex refractive index, which reduces propagation of light through the sensor. As the aluminum is removed, the power level will increase. The main objective of this sensor is to monitor aluminum corrosion.

2.0 HISTORICAL

Corrosion is a very serious factor that causes the degradation of metallic structures. Although metallic corrosion has many forms, a common factor in all mechanisms is the deterioration of a metal due to a chemical reaction with the surrounding environment. The natural state of a metal is the state in which the metal is found in the earth's crust, usually an oxide. Because the natural state of the metal is not used in industry, where the pure metal or metal alloys are typically used, corrosion occurs naturally. Therefore, whenever necessary constituents are present, corrosion occurs spontaneously.⁸ Some of the more detrimental results of corrosion are stress cracking and fatigue. Stress corrosion occurs when the material is weakened by the corrosion process, and normally occurring stresses cause the material to fail. The result is a crack in the material caused at much lower fatigue loading conditions than would be expected for the uncorroded metal. Corrosion fatigue is the failure of the material due to cyclic loading after it has been weakened by the corrosion process. The early detection of corrosion could prevent the two failure mechanisms from occurring.⁹

2.1 Corrosion detection techniques

There are currently many techniques to detect corrosion. Several of the most common methods are described below.¹⁰⁻¹⁵

Visual inspection: This is the simplest and most common method used to detect corrosion. Essentially, as the name suggests, a trained technician moves around the

structure and looks for evidence of corrosion damage. This method is costly, time consuming and often subject to human error.

Ultrasonic techniques: A high frequency wave is introduced into the material using an ultrasound transducer. This wave travels through the material, reflects off the far side, and travels back to the original transducer or a second transducer placed nearby. The time needed to travel through the material is used to determine the thickness of the material. This method can be used to monitor general thinning or localized thinning of the material. The problems with this technique are that the material must be homogenous and that layered materials will cause multiple reflections to return to the detector.

Eddy current examination: A coil with an ac current passing through it is placed near the surface of the structure to be monitored. Eddy currents form in the material near the coil and these eddy currents remain uniform unless there is a disturbance, such as a crack. Thin structures are best suited for this method because the depth of penetration is proportional to the frequency of the coil.

Neutron radiography: The material is irradiated with neutrons and a neutron detector is set up on the far side of the material. The attenuation of the beam is dependent on the amount of hydrogen present and, since hydrogen is a byproduct of corrosion, this method can be used to detect corrosion. This technique needs a radioactive source which increases the cost as well as the dangers of close proximity to humans. But the advantage of this method is the ability to detect corrosion in thick structures.

X-radiography: This technique involves the taking of x-rays of the structure, which can detect internal corrosion as well as general thinning of the material. The main problem with this technique involves the difficulty in interpreting the results of the x-rays due to varying thickness or uneven sealant and bonding surfaces of the material.

Acoustic emission techniques: Presently there are two types of acoustic emission sensors being implemented for corrosion monitoring. The first is an acoustic emission detector which is used to monitor the acoustic emissions that occur during the corrosion process. Unfortunately, only the more violent types of corrosion produce these acoustic emissions.

The second method involves the detection of damage after it has occurred. An external load is applied to the structure, and the acoustic emissions caused by this load are monitored. This method unfortunately necessitates the need for large loads on the structure and degradation to the structure caused by these loads.

Use of coupons: A coupon of the material of interest is placed with the permanent material and periodically removed for examination. This technique is mainly used in large industrial plants and each possible corrosion site in the structure would require an individual coupon.

Electrical resistance probes: The resistance of a material is directly proportional to its cross-sectional area. Therefore, monitoring the resistance of a material will give its cross-sectional area and the amount of corrosion the material has experienced. This technique

requires penetration of the material to insert the probes and this could create localized corrosion.

Hydrogen probe: The main byproduct of many corrosion processes is hydrogen. This probe consists of a thin foil, such as palladium attached to an electrolyte cell. The cell produces the current through the foil, which is required for the oxidation of the hydrogen. The current necessary for this reaction is measured and the corrosion rate is calculated from the current. The main disadvantage of this method is the necessity of high hydrogen diffusion rates through the material and the restriction to ambient temperature conditions.

Thus, all these above methods currently being implemented have many disadvantages. The main advantage of the fiber optic sensors proposed in this research is the ability to use these sensors as a continuous corrosion monitoring technique so that anti corrosion steps can be implemented as required. Fiber optic sensors have many advantages such as increased sensitivity and small size, as mentioned in the previous chapter. Fiber optic sensors also offer the advantage of the sensor not affecting its environment as well as the ability to embed the sensor to the required depth in the structure.

2.2 Aluminum-clad transmissive sensor

An aluminum-clad fiber sensor was studied for corrosion monitoring as a very simple and elegant method to solve the problem. There has not been another solution proposed with similar characteristics. The theory and experimental results are discussed in further sections.

2.3 Kretschmann Surface Plasmon Resonance Device

The Kretschmann prism for monitoring surface plasmon resonance is the basis for the surface plasmon sensor under consideration; with a view to producing a refractive index sensor, as well as a corrosion sensor. The assembly is named after E. Kretschmann, who along with A. Otto pioneered the technique in the late 1960s.¹⁶ Other applications of the surface plasmon resonance are discussed further in Section 2.4.

The phenomenon of surface plasmons has been well studied and summarized by Raether.¹⁷ Surface plasmons are the oscillations of the electrons that exist at the surface of a solid material containing free electrons. A plasma is generated in the free electron "cloud" on the surface of the conductor by the application of an external electric field to the boundary between the conductor and a dielectric.

The most used configuration to generate surface plasmon consists of a thin, planar conductive film that acts as the support for the plasmon. This film is surrounded on both sides by dielectric material. In order to support surface plasmons, the conductive material must have a dielectric constant with a real negative component. Many metals and semiconductors have dielectric functions containing a negative real portion, making them suitable materials for plasmon support.

Surface plasmons are obtained at optical frequencies by coupling guided or reflected electromagnetic waves to the free electrons on the conductive surface. The Kretschmann prism assembly is the time-tested method to produce surface plasmons. In this setup, a thin metal film, for example gold or silver, is deposited onto a surface of a highly refractive glass prism. The chemical of interest is also introduced over the thin metal film. A p-

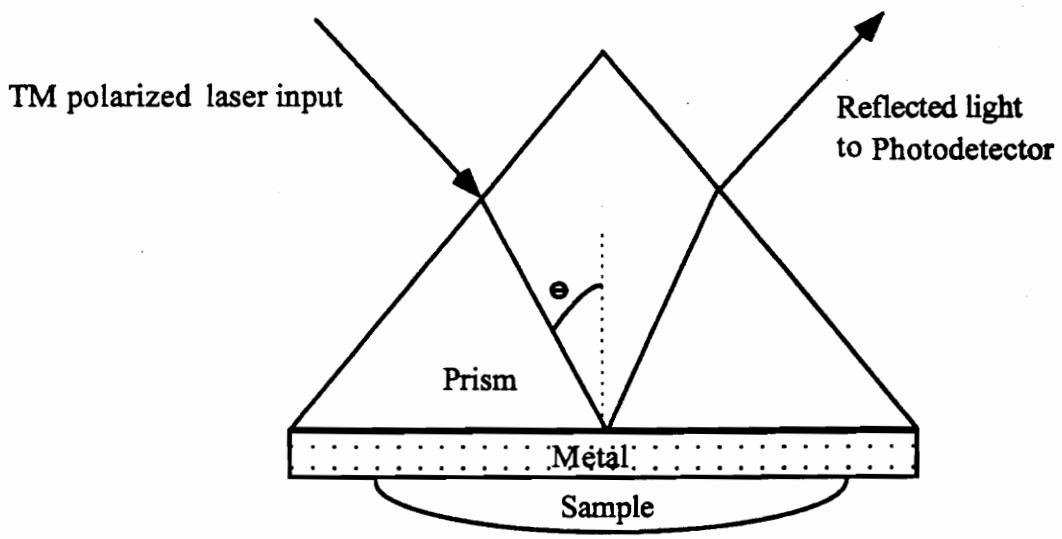


Figure 2.1. The Kretschmann prism configuration.

polarized light beam from a laser is launched through the prism as shown in Figure 2.1 and reflected from the prism/metal interface where a photodetector records the intensity of light.

2.4 Applications of Prism-Based SPR Devices:

Some of the earliest applications of surface plasmons were in the analysis of thin metal films. Surface plasmons were used to determine the dielectric constant and thickness of silver films by Robertson and Fullerton.¹⁸ Hyashi, *et al.* performed similar experiments but they monitored surface plasmon resonance due to surface roughness.¹⁹ Weber and McCarthy²⁰ used this technique to determine accurately the optical properties of gold, silver and copper films. Mao *et al.*²¹ used the prism SPR technique to measure the refractive index of amorphous rare earth transition metal compounds.

Detection of biological or biochemical molecules is the most widely used application of the prism-based SPR phenomenon. One member of the biochemical pair, for example a protein, is adsorbed onto the metal surface. If the biological conjugate of the protein, such as a specific antibody or enzyme, is introduced the reaction between the two will increase the amount of material at the surface of the metal. This increase in material causes an increase in the refractive index at the metal surface and a shift in the angle of minimum reflectivity for the surface plasmon. Since the plasmon is a surface effect, only materials within a few hundred nanometers of the metal surface will affect the generation of the plasmon. Thus, the substantial increase in surface bound material caused by the bioreaction causes an easily measurable change in the angle of minimum reflectivity. Liedberg, *et al.*²² applied a monolayer of the human immunoglobulin G to a silver film and measured the shift of angle of minimum reflectivity. Kooyman, *et al.*²³, used a similar

device to monitor the bioreaction between human serum albumin protein (HSA) and anti-HSA. Daniels, *et al.* ²⁴, monitored bioreactions between avidin and biotin as well as between alpha-feto protein (AFP) and anti-AFP. This device could monitor concentrations down to 10^{-8} molar range. In all the biosensors described above, the metal-coated surface of the prism acted as one side of a flow cell through which the samples of interest were introduced. Changes in laser launch angle were achieved either by rotating the prism or revolving the laser around the prism.

Another application of prism-based SPR devices is the determination of the optical constants of materials coated onto the metal surface of the sensor. Pockrand ²⁵ determined the refractive index as a function of thickness. Song, *et al.* ²⁶, detected very slight contamination of silver, aluminum, and copper surfaces and contamination in thin coatings.

These are some of the many applications of the prism-based SPR but they have been primarily of academic interest. Pharmacia Biosensor²⁷ has produced the only commercialized biosensing system using this principal. Their product is called BIAcore™ and costs over \$100,000 for a single prism-based system. Prism-based SPR devices provide relatively simple monitoring systems but they also require complex control of the laser and detecting equipment. Thus, they have not been widely used commercially. Fiber-based SPR devices are easier in that respect and were thus studied for corrosion monitoring.

2.5 Fiber Optic SPR Devices

Fiber optic surface plasmon sensors have been mainly utilized in the field of communications as a polarization device. Since surface plasmons are affected by only one component of EM waves (TM), they serve well to separate the TM and TE components selectively in an optical beam. They have been well tested as a polarization device by Johnstone, *et al.*²⁸, and Zervas²⁹.

Polarization maintenance is very important in coherent communications to avoid signal fading. The use of bulk optic components or integrated optics, as implemented in prism-based SPR devices, is not practical to provide polarization selectivity, since it increases cost and produces mechanical instability. Thus fiber-based SPR devices are more desirable as this ensures that the device is all fiber-based.

Fiber based SPR devices are constructed by polishing a small lateral section of the cladding to the evanescent field around the core. A thin coating of metal (30-50 nm) is deposited on the polished surface and the liquid of interest, with a specific refractive index, is introduced on the metal layer. This is the construction of the three layer SPR device, ie. fiber/metal/sample. A four layer SPR device also has been attempted.⁷

By the use of the proper metal with the required index, and thickness, and the liquid with the proper refractive index, surface plasmon resonance will be produced. The device under consideration in this research will deal mostly with the white light interactions on the fiber-based SPR sensor since this will produce a more broadband sensor. Figure 2.2 will illustrate the set up for a single wavelength SPR test as previously attempted by Bender.⁷ Although aluminum would be the ideal metal to apply as the metal layer because

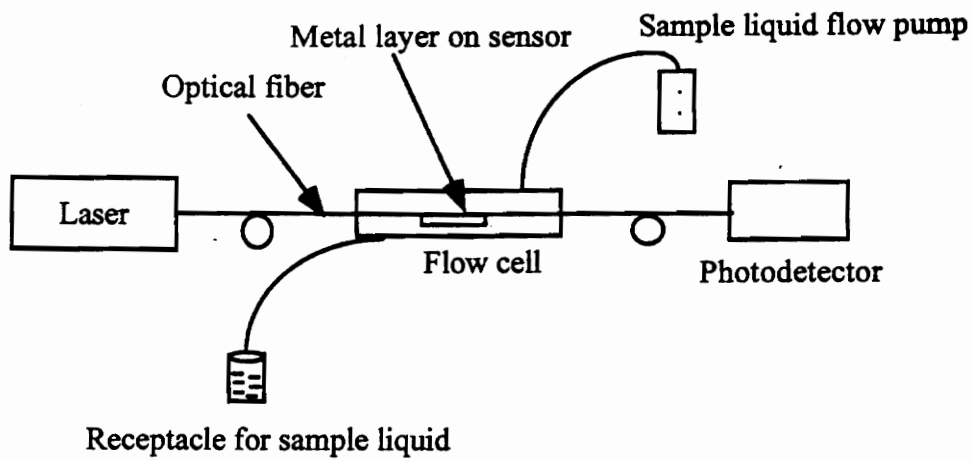


Figure 2.2. The setup for fiber based SPR sensors.

corrosion monitoring of aluminum structures is of specific interest, silver was attempted first as it possess the highest sensitivity.

Another similar fiber sensor has been recently proposed by Jorgenson *et al.*³⁰ for a surface plasmon resonance fiber optic based sensor for biochemical sensing. Their sensor is based on the multimode fiber and silver is used as the metal. Their results are very similar to results shown in Chapter 6 for the unpolished multimode SPR sensor. Jorgenson *et al.*³⁰ have also proven that their sensor can be utilized in a dip probe configuration for biochemical applications.

3.0 THEORY

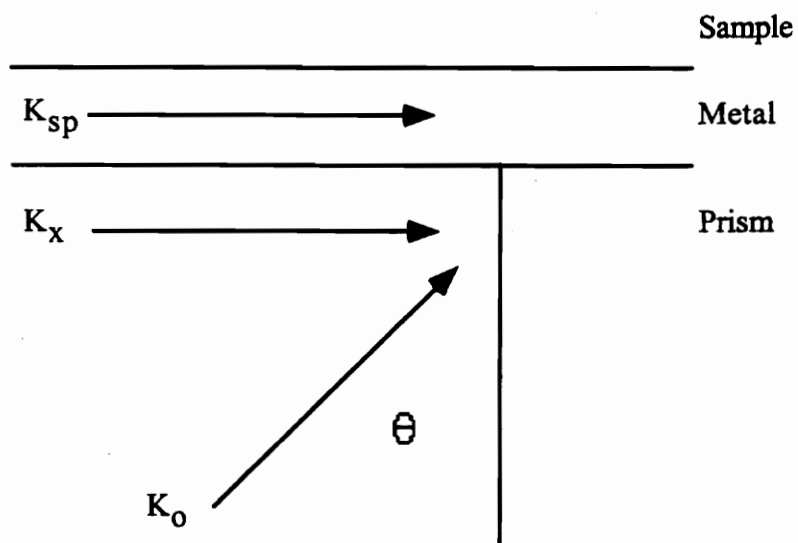
Theoretical studies of the SPR effect in both prisms and fibers serve well to predict the behavior of the devices. The mathematical description of the resonance condition in the prism relies on the use of wavevectors while the resonance condition in fibers is based on the dispersion equation.

Theoretical studies of the aluminum-clad fiber sensors are based on the evanescent theory and serve well to understand the working of the sensor for corrosion monitoring.

3.1 Theory of Prism-Based SPR Devices

Traditionally, SPR is measured using the Kretschmann configuration, as shown in Figure 2.1. The angle at which the minimum reflection intensity occurs θ is at the resonance angle in which coupling occurs between the incident laser light and the surface plasmon waves.

Wavevectors are used to describe the surface plasmon resonance condition in prisms. A wavevector describes the direction of propagation and the wavelength of a light wave⁷. For excitation of a surface plasmon, the x-component of the wavevector of the input laser light must match the wavevector of the surface plasmon in the metal. This condition is shown graphically in Figure 3.1 where Liedberg²² describes the wavevectors of the laser beam and plasmon. K_0 is the free space wavevector of the laser input beam. Thus, if the two expressions in Figure 3.1 are equated, the resonance condition can be predicted.



$$K_0 = 2\pi/\lambda$$

$$K_{sp} = K_0 \left(\frac{1}{n_s^2} + \frac{1}{n_m^2} \right)^{-1/2}$$

$$K_x = K_0 n_p \sin \theta$$

θ = angle of minimum reflectivity or resonance angle

Figure 3.1. Wavevector matching.

As shown in the Figure 3.1, for a given metal film, wavelength of operation of the laser and prism material, the refractive index of the sample liquid coated on the surface of the metal film and the angle of incidence of the laser beam generate the resonance condition. Small changes in the angle of incidence required to produce the resonance condition are caused by small changes in the refractive indices of the sample liquids. The angle that causes the resonance condition is called the angle of minimum reflectivity.

A fact to consider about the SPR technique is that it is a surface technique and hence, changes in the bulk solution on the metal film will not affect the process. The depth of penetration is called the plasmon sampling depth. Also, surface plasmon resonance cannot result from direct illumination of a metallic surface. The wavevector of the laser is always smaller than that of the plasmon. Thus, the existence of the glass prism is necessary in the arrangement to increase the laser's effective wavevector.

3.2 Theory of Fiber-Based SPR Devices

There are two possible configurations with the fiber-based SPR sensor; the three-layer and four-layer system. The three-layer system requires the metal layer to be deposited on the polished lateral surface of the fiber with the liquid sample coated on the metal layer. The three layers are fiber/ metal/sample. The four layer system consists of the polished lateral surface of the optical fiber coated with a metal and a dielectric overlay upon which the sample liquid is introduced. The addition of the overlay as will be shown later, allows a wider refractive index sensitivity. Thus, the four layers are fiber/metal/overlay/sample. The dispersion equation is used to predict the occurrence of surface plasmons knowing the refractive index and thickness of the considered three or four layers.

The choice of metal is very crucial in producing surface plasmons. As described by Bruijin *et al.*,³¹ the sensitivities for different metals vary with wavelength of operation. Silver has the highest sensitivity of any metal ($S = 41 \cdot 10^{-2} \text{ nm}^{-1}$) between 700-900 nm. Aluminum, on the other hand, has lower sensitivity with its higher values at the UV range of wavelengths ($S = 15 \cdot 10^{-2} \text{ nm}^{-1}$ at 300 nm and $S = 4.2 \cdot 10^{-2} \text{ nm}^{-1}$ at 700 nm). Thus, silver was chosen as the metal to study the effects of SPR resonances with white light interrogation. Aluminum will be attempted at a later date.

3.2.1 The Three Layer SPR System

The coordinate system used for the derivation of the dispersion equation of the three layer system is shown in Figure 3.2. The four factors that play an important role are the refractive index of the cladding, the metal and the sample, and the thickness of the metal layer. The effective index of the single mode and the wavelength of operation of the source are other variables in the dispersion equation.

The three layers are in the x direction while the direction of propagation of light is the z direction. The fiber/metal interface is arbitrarily chosen at $x = 0$ while $x = t$ implies the metal/sample interface as represented in Figure 3.2.

Bender⁷ derived the dispersion equation, assuming the following factors to simplify the process. The polished fiber is assumed to approximate a planar waveguide and the sample and cladding layers are assumed to extend to infinity in thickness. Even with these assumptions, their results are similar to those produced by Johnstone *et al.*²⁸ The Bender-Miller dispersion equation is shown below.³²

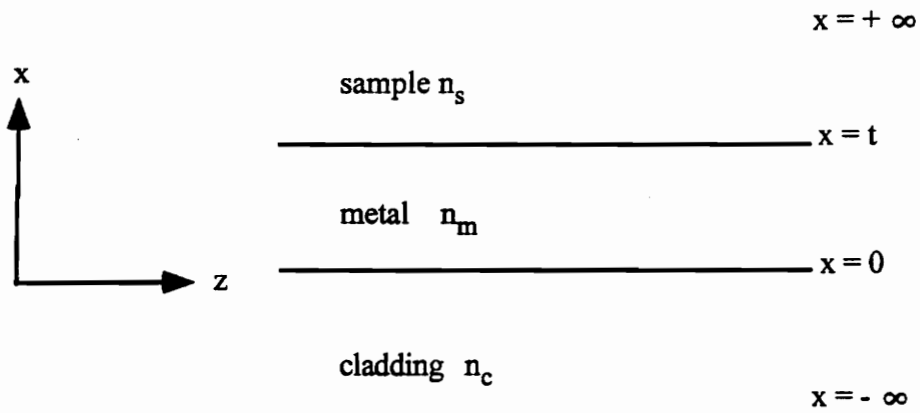


Figure 3.2. The three layer fiber SPR configuration.

$$t = \ln \left\{ \frac{\left(-\alpha^2/n_s^2 + \Delta/n_m^2 \right) \left(\rho/n_c^2 - \Delta/n_m^2 \right)}{\left(-\alpha^2/n_s^2 - \Delta/n_m^2 \right) \left(\rho/n_c^2 + \Delta/n_m^2 \right)} \right\} / 2\Delta \quad (3.1)$$

where t = thickness of the metal layer,

n_s = sample refractive index,

n_m = metal refractive index,

n_e = effective modal index,

$k = 2\pi/\lambda$,

$\beta = n_e k$,

$$\alpha = i(n_s^2 k^2 - \beta^2)^{1/2} = (\beta^2 - n_s^2 k^2)^{1/2}$$

$$\Delta = i(n_m^2 k^2 - \beta^2)^{1/2} = (\beta^2 - n_m^2 k^2)^{1/2}$$

$$\rho = i(n_c^2 k^2 - \beta^2)^{1/2} = (\beta^2 - n_m^2 k^2)^{1/2}$$

The dispersion equation as derived by Johnstone is also shown below.²⁸

$$k_0 t (n_e^2 - n_2^2)^{1/2} = \tanh^{-1}(A_1) + \tanh^{-1}(A_3) \quad (3.2)$$

$$\text{where } A_i = (n_2/n_i)^2 (n_e^2 - n_i^2)^{1/2} / (n_e^2 - n_2^2)^{1/2}$$

n_1 = cladding refractive index,

n_2 = metal refractive index,

n_3 = dielectric coating refractive index,

n_e = medal effective index,

$k_0 = 2\pi/\lambda$,

t = thickness of metal.

Using the results published by Bender⁷ and Johnstone *et al.*,²⁸ the above equations are used in all further analysis, as shown in Figure 3.3-3.5. The graphs are used from Reference 7 and 28 too.

In studying the theory of three layer fiber surface plasmon resonance, it was realized that the application of the sensors would be enhanced if it could be made to respond to a wide range of refractive indices. In previous experiments performed, a single wavelength source was used and thus with a certain thickness of metal deposition on the fiber, only a solution with specific refractive index would produce a resonance condition. This makes the sensor sensitive to only one index of refraction.

If a white light source was implemented instead of a single wavelength laser source, the above mentioned problem could be overcome. The range of wavelengths would produce many different resonance conditions that would produce sensitivity to different refractive indices. The sensor would be connected at the input to a white light source, while the output would be connected to a optical spectrum analyzer (OSA). When a solution of a specific refractive index is introduced, since all the wavelengths are present, a resonance condition will be produced which can be recognized because a peak will be produced at a certain wavelength at the OSA output. A theoretical output graph, Figure 3.6 is produced which represents the resonance points against the indices of the sample solution which will produce SPR. The metal used is silver which has a thickness of 44 nanometers. The fiber used is single mode at 1300 nanometers. The next graph, Figure 3.7 shows the theoretical resonance points if aluminum was chosen as the metal, using the same optical fiber.

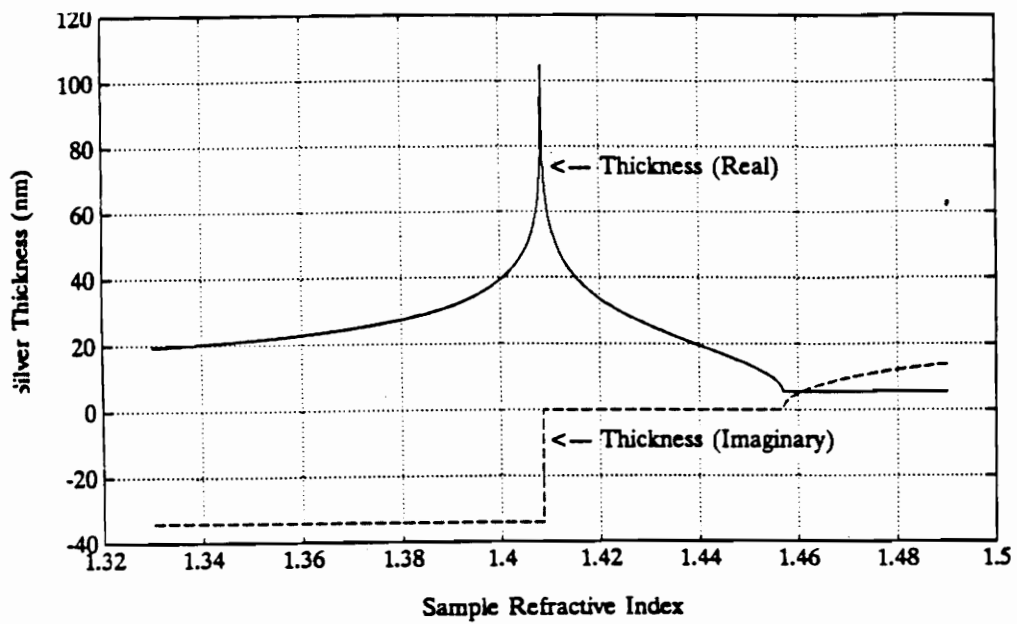


Figure 3.3. Dispersion plot of Bender equation.⁷

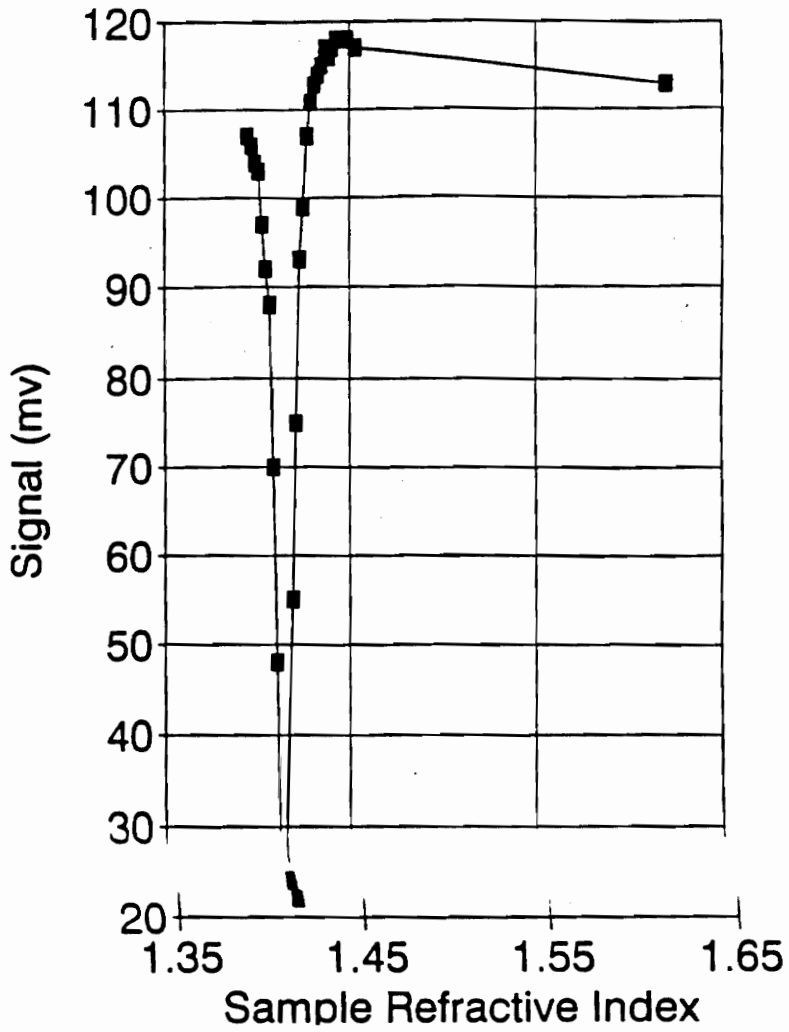


Figure 3.4. Experimental results of the Bender 3-layer SPR test.

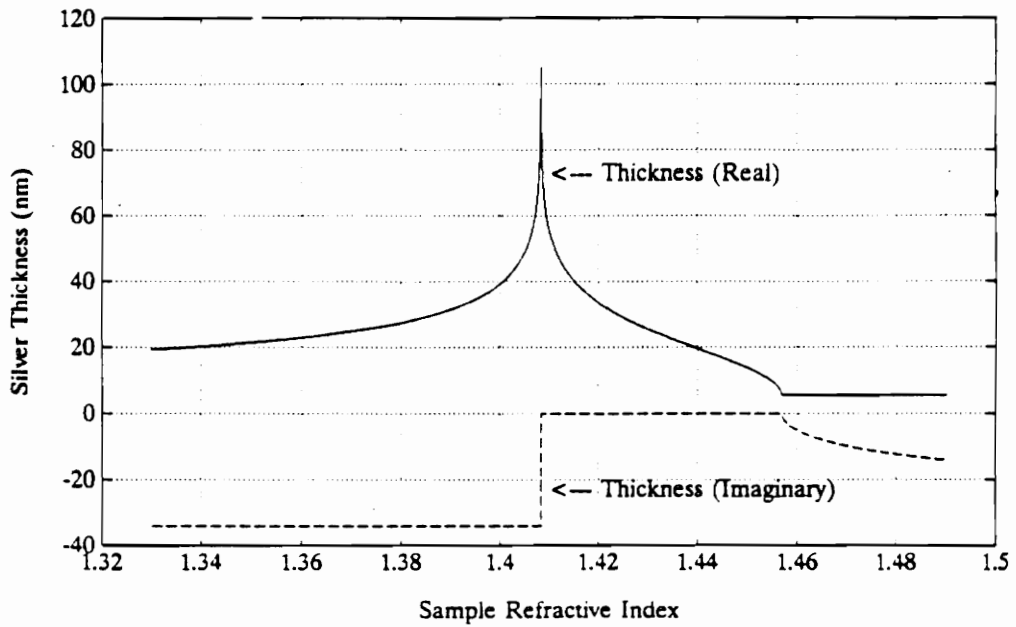


Figure 3.5. Dispersion Plot of Johnstone equation.²⁸

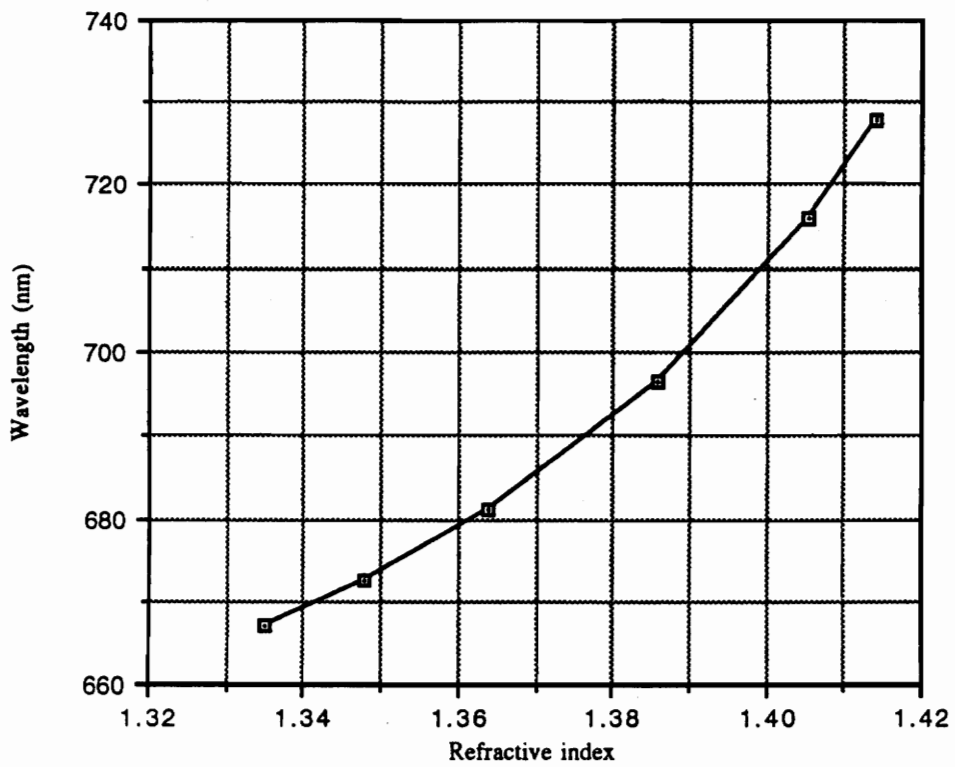


Figure 3.6. Theoretical response of three layer SPR sensor with silver overlay of thickness = 44 nm.

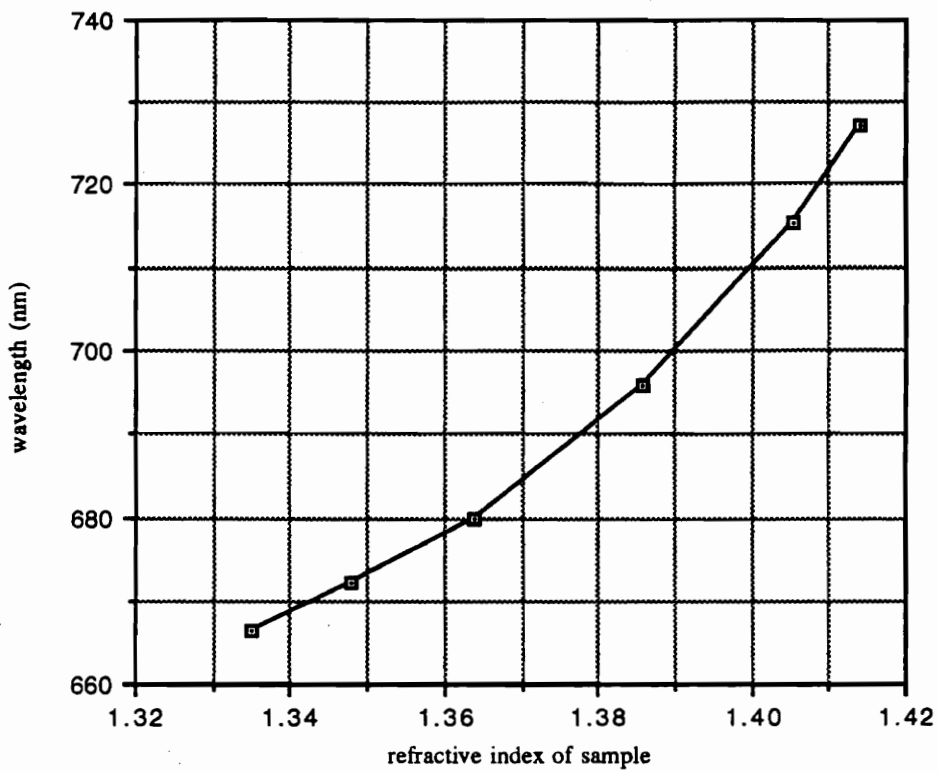


Figure 3.7 Theoretical response of three layer SPR sensor with aluminum overlay of thickness = 44 nm.

The optical fiber used in the above case was a single mode but another configuration was attempted where multimode optical fiber SPR sensor was implemented. The multimode fiber was used as the sensing fiber to increase the throughput of the sensor and reduce fabrication time. Since the multimode fibers have larger numerical apertures, they allow more light to propagate through the fiber, which increases the throughput of the sensor and reduces noise. The multimode SPR sensors were constructed using two methods. One of the ways entailed polishing the fibers in a similar manner to the fabrication of the single mode SPR sensor. This method made use of the evanescent field of the core that permeates into the cladding, as in the single mode case. Another fabrication method involved the total removal of the cladding and deposition of the metal on the core of the fiber. This method makes use of the reflections on the core/cladding surface of a multimode fiber. Since a multimode fiber has many modes, all the modes propagate along the fiber with reflections along the surface of the core. When these reflections come in contact with the metal layer at the surface of the core of the fiber the light is attenuated, depending on the refractive index of the sample liquid on the surface of the metal layer. This method of fabricating the surface plasmon sensor is relatively simpler because removing the cladding is easier than polishing a fiber to the evanescent field.

3.2.2 The Four Layer SPR System

Due to inherent limitations of the three layer system, a four layer system was attempted by Bender and was successively implemented. Figure 3.8 shows its configuration.

The three layer system was limited in its range of operation. In order to understand this limitation, the concept of effective index should be explained clearly. In order to be able

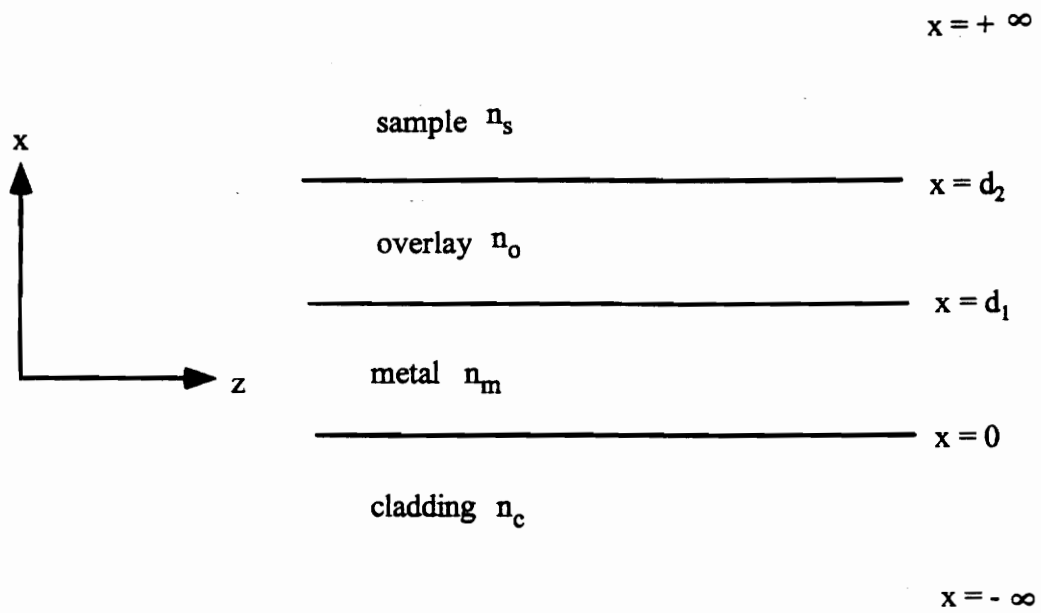


Figure 3.8. The four layer fiber spr configuration.

to generate surface plasmons, the effective index of the single mode propagating in the fiber should be approximately matched to the effective index of the layer deposited on the metal. This in turn, depends on the refractive index and thickness up to the first few hundred nanometers of the sample liquid. Thus the three layer is limited in its range of operation because by using just one layer above the metal, low refractive indices cannot be detected. Thus, lower refractive indices can be detected by increasing the refractive index of the layer above the metal by introducing a very thin dielectric layer with a high refractive index between the sample and metal layer. It was very necessary to detect lower refractive indices in order for Bender to construct a useful chemical sensor. The dispersion equation was also derived by Bender-Miller for this scenario too in a very similar manner to that for the three layer system. The graphs are also attached (Figures 3.9-3.10).

$$d_2 = \ln \left\{ \frac{ \left[\frac{\Delta}{n_m^2} + \frac{\rho}{n_c^2} \right] \left[e^{(\gamma+\Delta)d_1} \right] \left[\frac{\gamma}{n_o^2} - \frac{\Delta}{n_m^2} \right] - \left[\frac{\rho}{n_c^2} - \frac{\Delta}{n_m^2} \right] \left[e^{(\gamma-\Delta)d_1} \right] \left[\frac{\gamma}{n_o^2} + \frac{\Delta}{n_m^2} \right] }{ \left[\frac{\rho}{n_c^2} - \frac{\Delta}{n_m^2} \right] \left[e^{-(\gamma+\Delta)d_1} \right] \left[\frac{\Delta}{n_m^2} - \frac{\rho}{n_o^2} \right] \left[\gamma \right] + \left[\frac{\Delta}{n_m^2} + \frac{\rho}{n_c^2} \right] \left[e^{(\Delta-\gamma)d_1} \right] \left[\gamma \right] \left[\frac{\gamma}{n_o^2} + \frac{\Delta}{n_m^2} \right] } \right\} / 2\gamma \quad (3.12)$$

where n_s = sample refractive index,

n_m = metal refractive index,

n_e = effective modal index,

n_o = overlay refractive index

$k = 2\pi/\lambda$,

$\beta = n_e k$

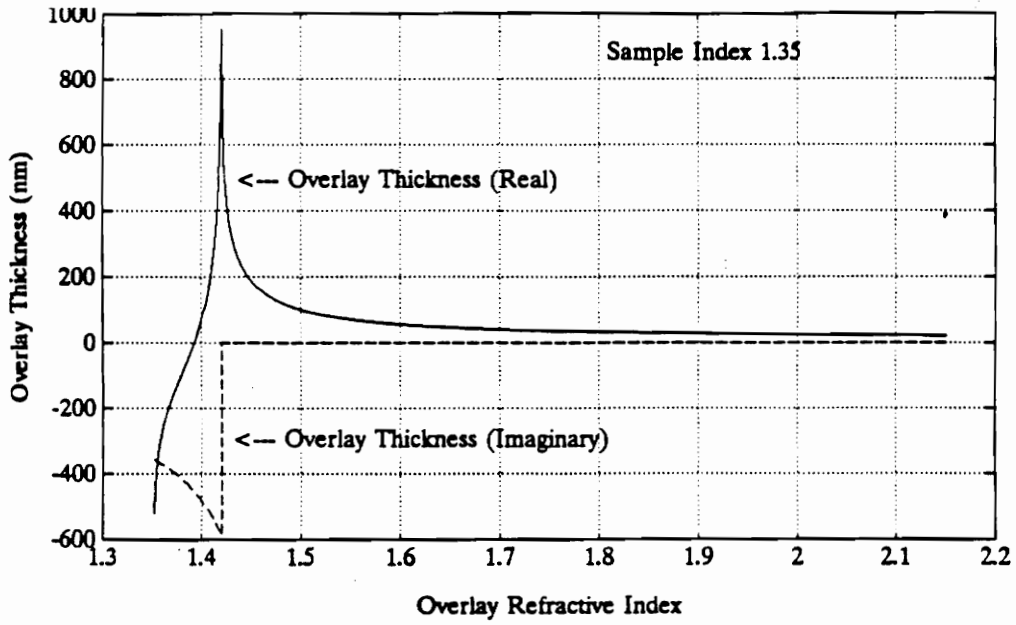


Figure 3.9 Dispersion of the Bender-Miller equation.³²

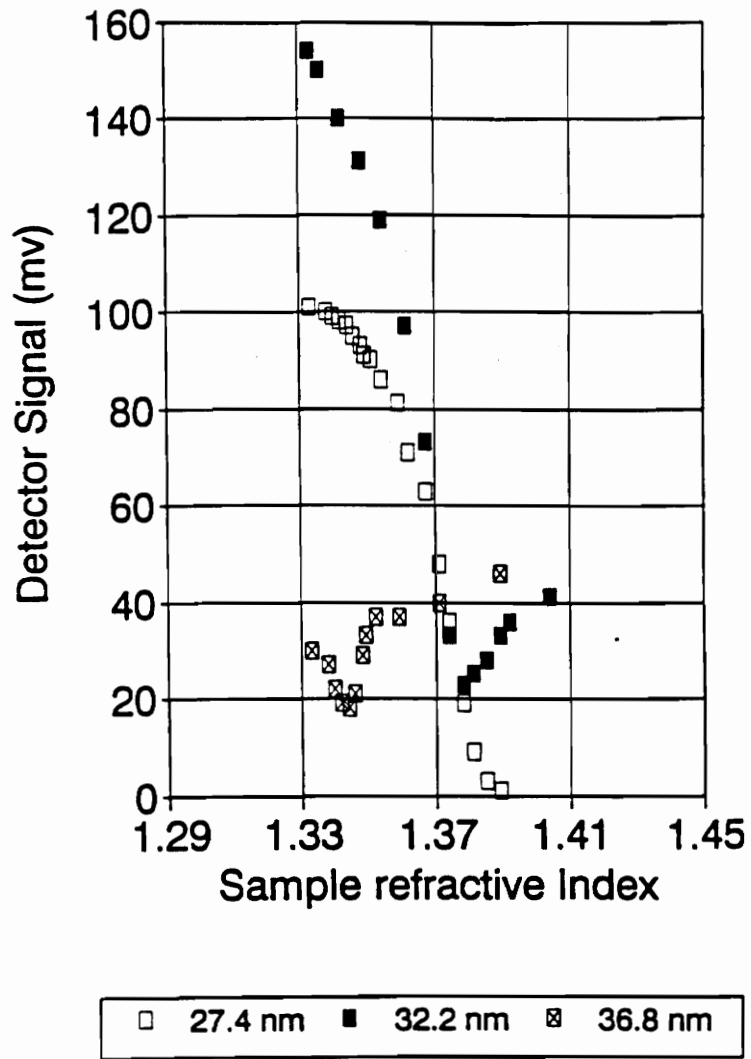


Figure 3.10 Results of the four layer experiment.⁷

$$\alpha = i(n_s^2 k^2 - \beta^2)^{1/2} = (\beta^2 - n_s^2 k^2)^{1/2}$$

$$\Delta = i(n_m^2 k^2 - \beta^2)^{1/2} = (\beta^2 - n_m^2 k^2)^{1/2}$$

$$\rho = i(n_c^2 k^2 - \beta^2)^{1/2} = (\beta^2 - n_m^2 k^2)^{1/2}$$

$$\gamma = i(n_o^2 k^2 - \beta^2)^{1/2} = (\beta^2 - n_o^2 k^2)^{1/2}.$$

A white light interrogation of the four layer surface plasmon was not attempted because it is not useful in increasing the sensitivity of the sensor. With the white interrogation of the sensor, a broad range of refractive indices can be detected.

3.3 The Transmissive Aluminum-Clad Fiber Corrosion Sensor System

There are two possible methods for employing a transmissive optical fiber sensor to monitor corrosion. First, a conventional optical fiber can be coated with a metal instead of standard polymeric coatings. Changes in the metal coating could cause changes in the light field propagating down the fiber. Since most optical fibers are designed to tightly confine the light in the core of the fiber, this technique might not be the most effective method for monitoring corrosion. A second, and possibly better, method is to replace the standard core/cladding geometry with a glass core and metal cladding which causes interaction between the light in the core and metal cladding. As anticipated, the aluminum-coated fibers did not show an appreciable response to corrosion because the electromagnetic field for a standard fiber is tightly confined to the core. Corrosion-induced changes in the aluminum coating did not appear to have a significant affect on the level of propagation of the light along the fiber.

It was decided to be use the aluminum-clad fiber sensor as a means to detect corrosion. This type of sensor is considered an averaging type sensor. The sensor will give an output signal value which represents an average measurement over the length of the sensing region. Therefore, if information about a specific location is needed, a modification to the sensor may be required and this aspect is discussed in Chapter 7.

The fiber was specially manufactured by Fiberguide with a glass core diameter of 140 μm and 180 μm cladding diameter of aluminum. Cutback tests were performed to determine the loss per unit length of the aluminum-clad fiber. The losses per unit length is required to determine the optimal length of the aluminum-clad fiber utilized to produce a reasonable change in output power level due to corrosion-induced aluminum clad loss. The aluminum-clad fiber was spliced to the polyimide coated as shown in Figure 3.11. The output from a 633 nanometers HeNe laser source was injected into the polyimide coated fiber and through the splice into the aluminum-clad fiber. After the initial power level was registered, the aluminum-clad fiber was cut back approximately an inch at a time, and the resulting output power levels were noted, the results have been tabulated in Table 1. As can be seen, the relationship between the output power and time is approximately linear. Since the relationship is reasonably linear, it is recognized that any length of aluminum-clad fiber could be used. The point to remember is that the longer the length of aluminum-clad fiber, the more will be the inherent loss of the sensor. As can be seen in Chapter 5, many different lengths of fibers were used to make corrosion sensors.

The aluminum-clad fiber sensor (construction is explained in Chapter 4) was tested using sodium hydroxide (NaOH) to simulate the process of corrosion. The input end of the corrosion sensor was connected to a laser source and the output end to an optical power

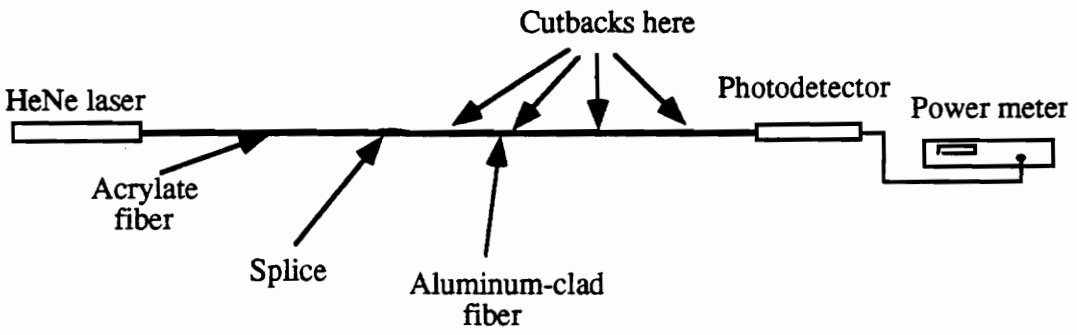


Figure 3.11. The setup of the "cutback" test.

Table 1. Data from the "cutback" test.

Fiberguide		Hughes	
Length(in)	Output Power (dBm)	Length (in)	Output power (dBm)
4.957	-16.300	8.000	-23.900
3.720	-14.700	6.750	-19.000
2.900	-11.300	5.750	-17.600
1.405	-9.200	4.500	-14.700
0.864	-6.300	4.000	-13.800
0.040	-6.000	3.000	-12.400
		2.250	-8.900
		1.250	-6.800
		0.500	-5.200
		0.200	-4.500

Input power for Fiberguide splice = 0.25 dBm

Input power for Hughes splice = -1.9 dBm

meter. The real part of the refractive index of aluminum is much larger than that of glass. The large difference at the interface of the aluminum-clad sensor fiber thus will result in very different light guiding characteristics than those observed for conventional communication-grade fiber. Aluminum also has a complex index of refraction, which causes loss. In the aluminum-clad fiber, the lower order modes in the core are highly confined while the higher order modes are affected by the metal coating on the fiber. Hence, if the fiber is bent, a part of the lower order modes is coupled into higher order modes and subsequently stripped away by the aluminum, thereby causing loss. In practice, bending loss is a problem and should be taken into consideration when laying out the sensor on a structure; if the sensor is kept straight, the corresponding loss will be small.

The sensors will be immersed in a container of NaOH and the output monitored by an optical power meter. The power level would initially remain constant because the light in the core extends only a certain distance into the metal cladding. Typically, for aluminum, the skin depth or evanescent region is between 5 to 10 μm . Since the cladding thickness started at 20 μm , it would take a certain amount of etching before the light field would experience a change in material parameters and thickness caused by corrosion. At the point when the aluminum thickness equals the skin depth (or the evanescent field of the core was penetrated), the NaOH, with an index of refraction of 1.41, forms a secondary cladding. This secondary cladding acts more like a proper waveguide, and hence the power level should increase continually as the remainder of the aluminum etches away. The amount of power level rise cannot be predicted as it depends on the wavelength of the source and differences in the angle of incidence between the fibers at the splice.

4.0 SENSOR CONSTRUCTION

The method of constructing both the surface plasmon sensors and transmissive aluminum-clad fiber sensor is discussed. Both sensors require time and considerable effort to construct. The corrosion sensor requires the sensing length of aluminum-clad fiber to be spliced to multimode fiber on both ends. The three layer SPR sensor requires the fiber to be bonded to a substrate and polished to the evanescent field of the core when a metal layer is deposited.

4.1 Three Layer Surface Plasmon Sensor

The three layer SPR sensor was constructed using Corning 1300 nm single mode fiber. Approximately 5 cm of the fiber jacket was removed from the central length of about 0.6 meters of fiber. The stripped portion of the fiber is then bonded to a polishing substrate using fingernail hardener and allowed to cure for 24 hours. The polishing substrate is a piece of aluminum approximately 5 cm long, 1.25 cm in height and 0.3 cm wide. The top surface of the fiber is curved along the length of the substrate so that its height is only 2.2 cm at the ends.

After the fiber is suitably bonded to the surface of the substrate, the ends of the fiber are cleaved. The fiber is now ready to be polished. The aim of the polishing procedure is to remove a short section of the fiber's cladding so that the evanescent field around the core of the fiber can be reached. This procedure is very imprecise because although the polishing technique should remove the cladding, it should not reach the core. The polishing procedure is followed by connecting one end of the fiber to a laser source of

1300 nm and the receiving end to an optical power meter. The output power is monitored continuously and carefully to insure the core of the fiber is not penetrated.

The polishing is done using a Buehler Corporation polishing wheel and a 1 μm grit polishing pad. The polishing substrate with the attached fiber is mounted onto a small cart built by Bender.⁷ This cart is gently moved back and forth over the polishing pad which is rotated. The procedure is continued using an optical power meter to continuously monitor the output power. The polishing procedure is terminated when the output power drops significantly, indicating that the pad has penetrated the evanescent field of the fiber. This state is also confirmed by lifting the substrate from the polishing pad and dropping a liquid of refractive index considerably larger than water (for example glycerol) which causes a tremendous drop in power. Upon flushing the liquid with higher refractive index with water, the original dropped power is obtained. The polishing procedure is now complete. If the polishing procedure is overextended and the core of the fiber is penetrated, the amount of light seen at the photodetector would be drastically reduced. The whole procedure from bonding the fiber to the substrate will then have to be repeated. Figure 4.1 shows the polishing setup and a simple schematic of the sensor configuration.

The fiber is now ready for the deposition of a metal layer. Silver was deposited onto the polished surface of the fiber using a vacuum vapor deposition chamber as described by Bender.⁷ Appropriate thickness of deposition are chosen depending on the fiber being used. In this case 44 nm of silver was deposited because 1300 nm fiber was used. A graph as shown in Figure 4.2 shows the thickness versus wavelength dependence derived from the Bender-Miller equations.³²

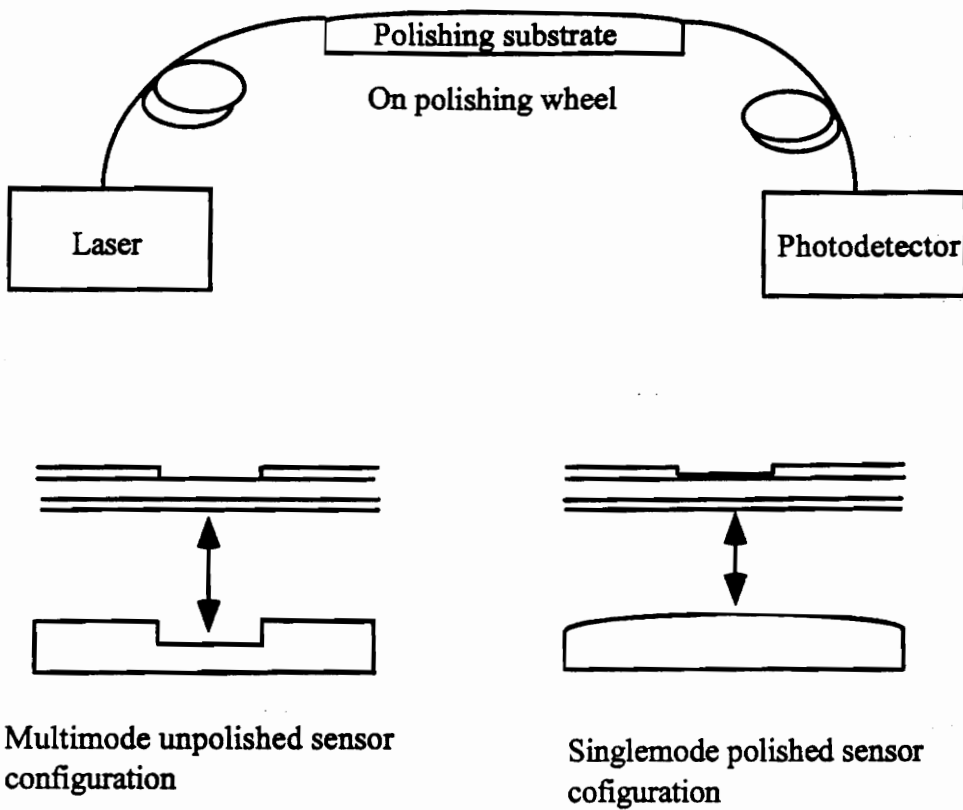


Figure 4.1. Schematic of the polishing setup for 3-layer SPR sensors and configuration of the single mode and multimode sensors.

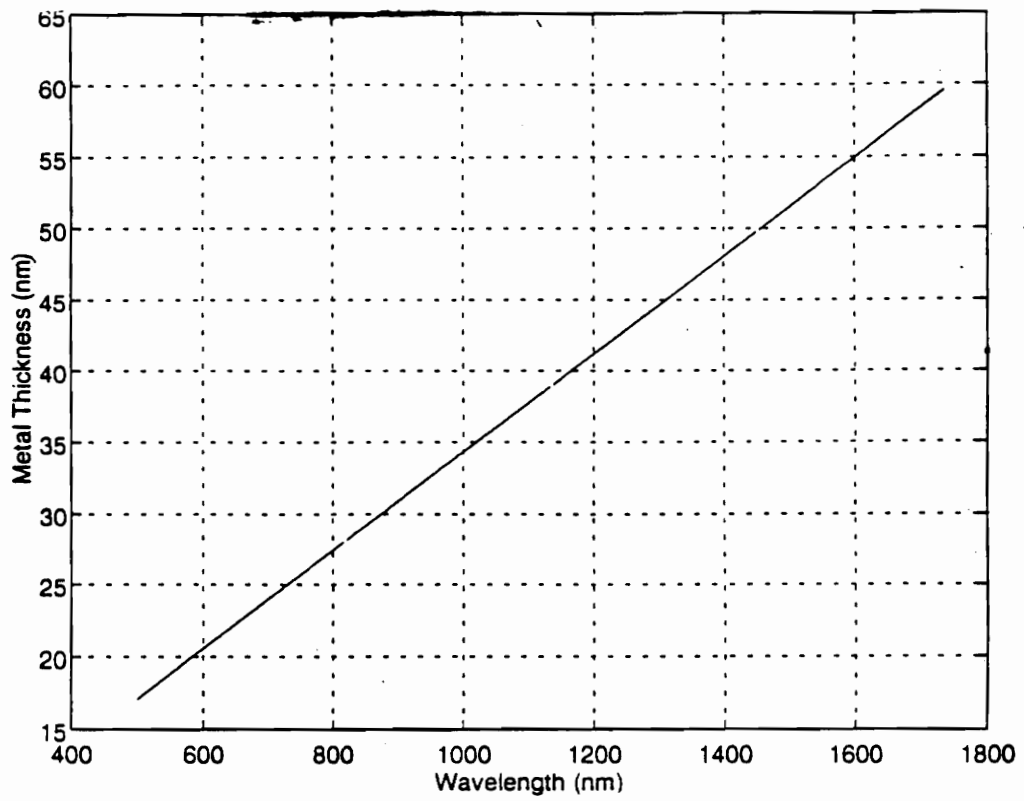


Figure 4.2. Wavelength vs. refractive index dependence of the 3-layer configuration.

Another configuration of the fiber-based SPR sensor was attempted because of lack of large throughput of light through the single mode fiber sensor. This sensor was fabricated using multimode fiber. In the first method, a similar concept was used as the single mode sensor where the fiber was polished down to the evanescent field of the core and a metal layer was deposited. This setup did increase the throughput of the sensor considerably and the noise at the output was decreased significantly. The fiber used for this configuration was a 1300 nm step index multimode fiber. A step index multimode fiber was used because the refractive index of the core and the cladding are known for the analysis of the response unlike a graded index fiber. The other method was to completely remove the cladding of a section of the fiber and have the metal deposited on the core of the optical fiber. In this configuration, the reflections of the different modes at the core/cladding interface interact with the metal layer to produce surface plasmon attenuation. This is the method also produced by Jorgenson *et al.*³⁰ This configuration also considerable increased the throughput of the sensor. The fiber used in this case was a 200/240 step index multimode fiber. The cladding was removed simply by scraping the surface of the fiber with a blade. Considerable care was taken to ensure that all the cladding was removed at the section of the fiber where the metal was to be deposited.

4.2 Transmissive Aluminum-Clad Fiber Sensor

The transmissive aluminum-clad fiber sensor is fabricated using the following specifications. The sensing length used is the 140 (core)/180 (cladding) μm aluminum-clad fiber diameter from Fiberguide with an acrylate coated 100 (core)/140 (cladding) μm multimode fiber on either end. The hollow core had inner diameter of 145 μm . The epoxies used to adhere to the hollow core fiber is Devcon 5-minute epoxy as well as cyanoacrylate epoxy.

The corrosion sensor is fabricated by using the following procedure. Etch the two ends of the sensing length of the aluminum-clad fiber using an etchant, for example sodium hydroxide (NaOH). Immerse 1.25 cm inch on either end to leave 2.5 -7.5 cm of sensing length as required. Cleave its ends. Strip the coating of the multimode fiber (approximately 1.25 cm) and cleave its ends. Inject light into the multimode fiber using a laser source of required wavelength (633 nm, 850 nm or 1300 nm) and using a optical power meter, note the amount of output power at the end of the multimode power as a reference. Strip the coating from a section of hollow-core fiber and cleave both ends with a blunt scribe. The length of the hollow core fiber should be so chosen to agree approximately with the length of the stripped multimode fiber and the etched aluminum-clad fiber sensor.

Align the cleaved multimode fiber to the hollow core fiber using an aligning setup. The multimode fiber is inserted carefully into the hollow core fiber until all of the stripped portion is inside it. If any of the stripped portion is not inside the hollow core tube, it will weaken the sensor mechanically and cause it to break easily. The fiber will not go in any further than the stripped portion because the outer diameter of the multimode fiber is much larger than that of the hollow core tube. Put 1 drop of cyanoacrylate epoxy to epoxy the multimode onto the hollow core fiber. After that it is dry in 2-3 minutes, put 3-4 drops of Devcon epoxy over it to further strengthen the bond. Let the epoxy cure for 5 minutes. Repeat this procedure for another length of multimode fiber to be epoxied to another piece of hollow core fiber.

Apply a small amount of index matching liquid to the end of the cleaved aluminum-clad fiber. Align the aluminum-clad fiber in the hollow core fiber to the multimode fiber glued to epoxy to the other end until the ends of the fibers just barely touch. Use the positioners to optimize the alignment. Epoxy as before using both epoxies. After waiting for the appropriate time to make sure the epoxy is fully cured, repeat the same procedure for the other end of the aluminum-clad fiber sensor to be epoxied to the other multimode fiber in the hollow core fiber. Optimize this alignment by monitoring the output power at the end of the multimode fiber using the optical power meter. A glass tube of inner diameter 300 μ m can be inserted over each spliced section to provide mechanical stability. Figure 4.3 shows a schematic representation of the aluminum-clad fiber sensor.

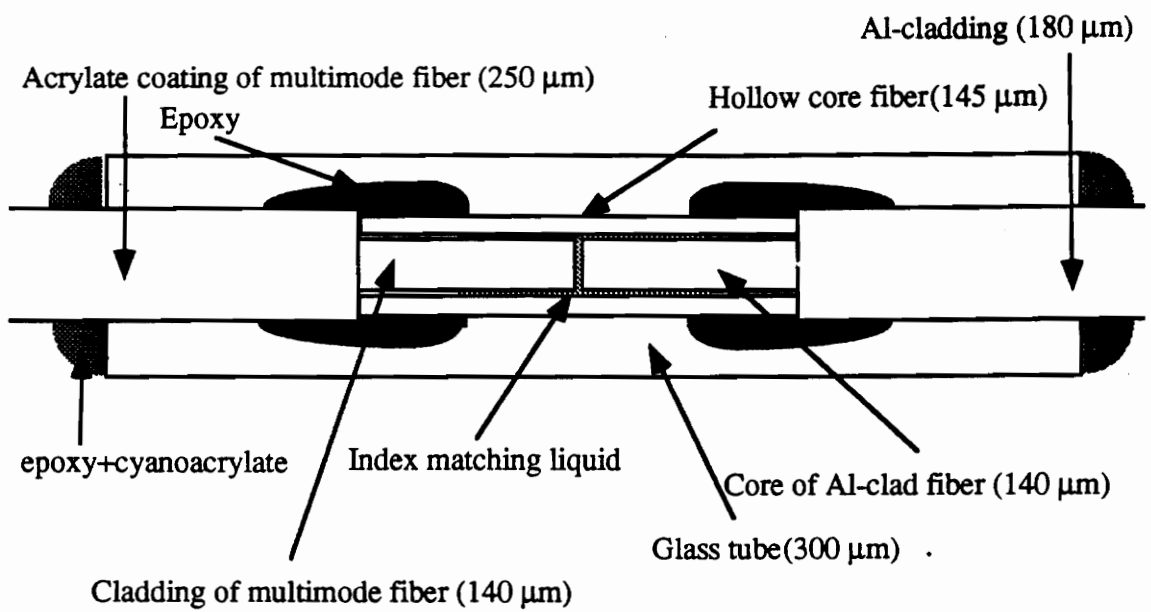


Figure 4.3. The splice of aluminum-clad and multimode fiber.

5.0 EXPERIMENTAL SETUP

In implementing the SPR and transmissive aluminum-clad fiber sensors for corrosion monitoring, tests were performed to validate the theory proposed in the previous chapters. Diagrams of the experimental setup are shown.

5.1 Experimental setup of the prism SPR sensors

Some simple experiments were performed with the Kretschmann prism assembly to gain an understanding of the theory of surface plasmon resonance.

The prism assembly consists of a silver-coated microscope slide that is placed in optical contact by an index matching liquid to a glass prism. The microscope slide, the index matching fluid and the glass prism have identical indices of refraction so that the glass prism can be used in repeated experiments with different metal-coated slides. The thickness of the silver coating on the slide is approximately 55 nm which is an accepted value as suggested by many research journals. A large, semicircular aluminum-plate goniometer was constructed to allow scanning of the laser beam over a wide range of launch angles into the prism. The launch angle of the laser source is measured with a tapered point on the end of the laser swing arm which in turn points to an angular scale that is marked on the circumference of the plate. The other end of the swing of the laser holds the photodetector. The glass prism is mounted on a common pivotal arm of the swing arms with a magnetic base. It also has a brass rod that threads into the rear of a flowcell which is filled with the required sample.

The optical source used was a 780 nm laser. Sucrose solutions varying in concentration to have different indices of refraction were made by dissolving the sucrose in distilled water in a volumetric flask, then diluting to the appropriate mark with distilled water. The solutions were sequentially applied to the sensor surface of the glass prism via the flow cell. The laser is then moved around on its pivot and the optical output signal reaching the photodetector is recorded for a range of laser launch angles. The plot of laser intensity reaching the detector as a function of laser launch angles is called the surface plasmon resonance profile.

The measured launch angle differs from the angle measured from the angle striking the prism/metal interface because of the refraction at the air/prism interface and the angle between the prism/metal interface and the goniometer endline. This arrangement is used because the angle needed to produce surface plasmon resonance is approximately 68° , which cannot be achieved if the hypotenuse of the prism is aligned with the goniometer endline. This arises because of the refraction of the laser beam as it passes from the low refractive index air around the prism into the highly refractive prism. Measuring the launch angle of the beam with the goniometer scale is as valid as measuring the actual angle at the prism/silver interface.⁷

Figure 5-1 shows the setup of the prism SPR experiment. Increased concentration of sucrose which in turn implies an increase in refractive index of the solution causes a shift in the angle of minimum refractivity. The data and plots are shown in the next chapter.

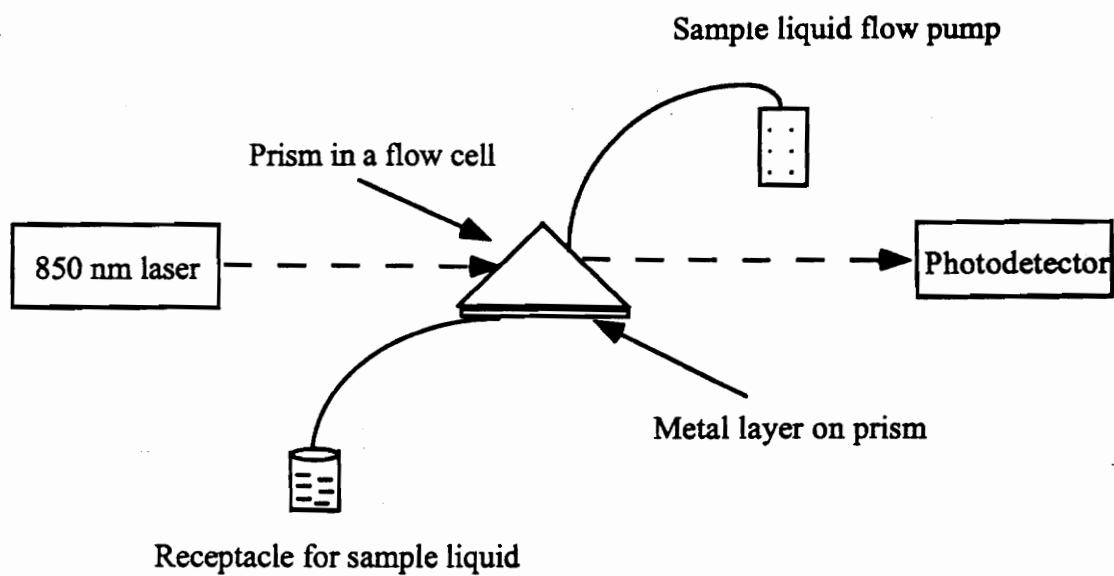


Figure 5.1. The setup for prism based SPR sensors.

5.2 Experimental Setup of Fiber SPR Sensors

As described in Chapter 3 and 4, a three layer SPR sensor was manufactured and tested using a white light source. The instrumentation used to carry out the fiber-based experimentation consists of a white light source, a flowcell to house the active portion of the sensor and allow the introduction of chemical samples by means of a pump and an optical spectrum analyzer (OSA). The schematic is presented in Figure 5.2.

The white light source used is a tungsten lamp housed in a metal casing. The OSA is a spectrum analyzer that allows the introduction of a fiber end directly by the use of a fiber chuck. The range of the OSA is from 450 to 1700 nm. Since the polishing substrate and fiber remain together throughout the testing of the fiber, a flowcell was designed to accommodate both the fiber and substrate. The flowcell is made of Plexiglas and uses two threaded tubing attachments to allow the introduction and removal of chemical samples. When a sample is introduced into the flowcell, the entire active sensing length of the fiber is surrounded by it. Since it is hard to align a polarizer to a white light source, it was not possible to polarize it. As mentioned before, surface plasmons are only affected by TM polarization.

The three layer fiber sensor was tested by the sequential application of fluids of known refractive indices. When the sensor was appropriately immersed in the solution, the optical throughput was recorded on the OSA. The flowcell was then flushed with water and enough of the next solution was allowed to flow through to negate any remaining effects of the previously applied solution. In the first few experiments performed, 44 nm of silver was applied. Solutions with refractive indices 1.3350-1.4062 were introduced.

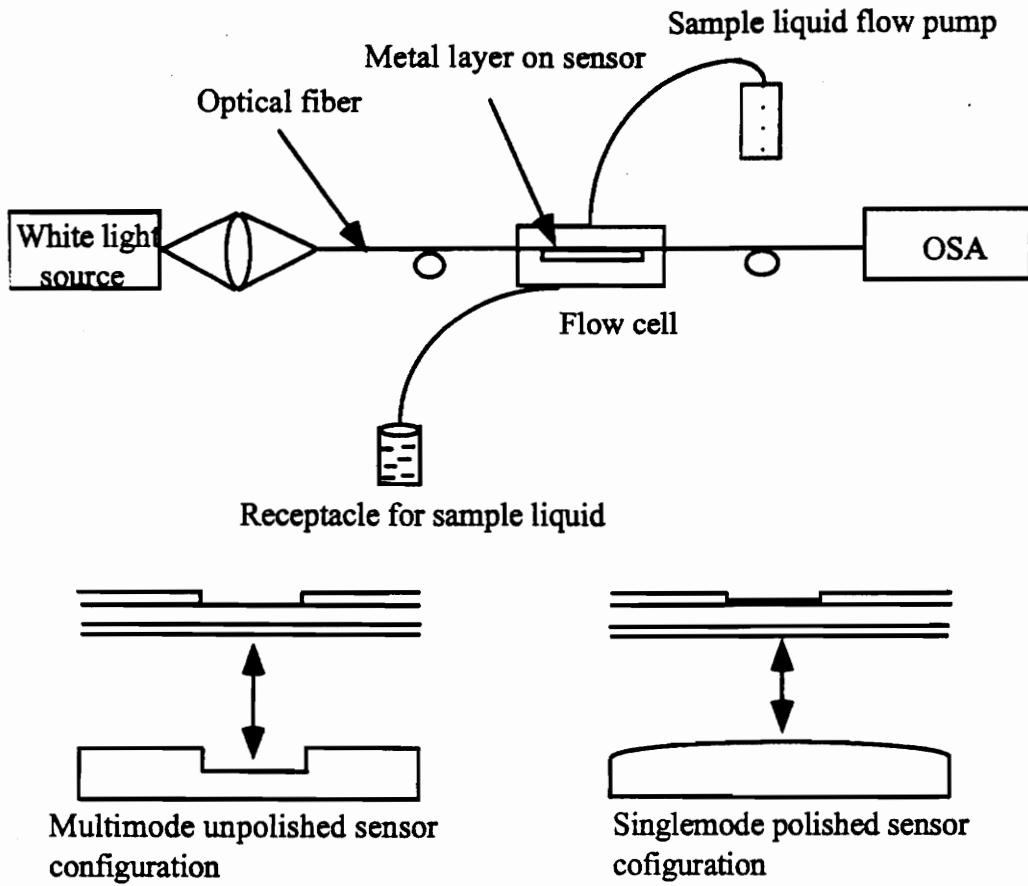


Figure 5.2 The setup for fiber based spr sensors.

Plots and tables of results are shown in the next chapter. Since the throughput of the sensor was not large enough, it produced a noisy spectrum at the OSA. A similar arrangement was setup with the polished and unpolished multimode sensors and different refractive index solutions were introduced. The spectrum at the OSA was significantly less noisy and reproducible results were obtained.

5.3 Aluminum-Clad Transmissive Sensor

The aluminum-clad sensor was tested for corrosion using Sodium Hydroxide (NaOH) to determine how much of the aluminum had to corrode in order to have a change in the output power as predicted by the theory. Since corrosion is a long and slow process, NaOH was used to etch the fiber to simulate the process in a shorter period of time.

A HeNe laser or a 1300 nm laser were used as the source of light. A 850 nm LED was also used to perform some of the experiments. Figure 5.3 shows the setup for the NaOH tests. The output fiber was fed into a detector/power meter. The aluminum-clad fiber was immersed in the solution of NaOH and the optical output power was monitored every minute until the aluminum cladding of the sensor fiber was completely etched.

During testing, optical loss was also observed when the aluminum-clad fiber orientation was altered. The output power level changed drastically as the sensor fiber's shape was altered. As explained in the previous chapter, this caused by bending loss. Therefore, care was taken to place the sensor as straight as possible in the NaOH bath.

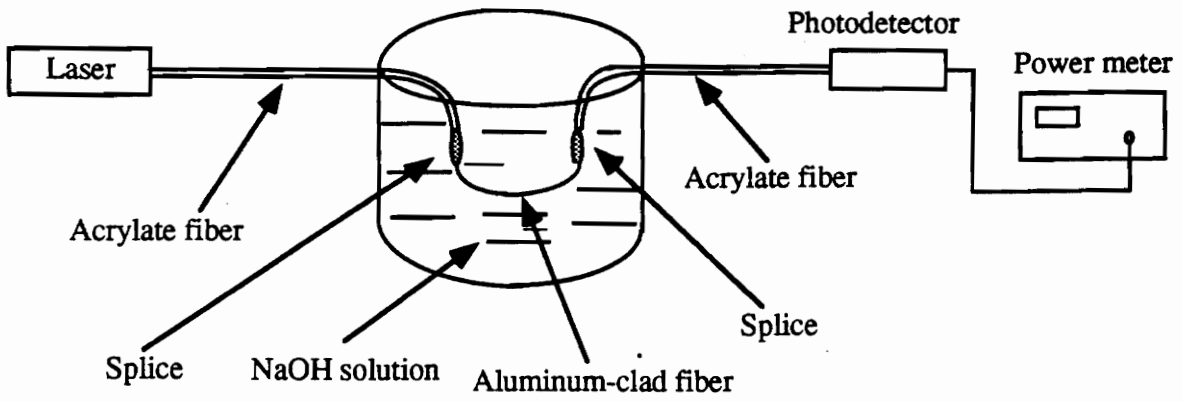


Figure 5.3. The setup of the NaOH etch test with the aluminum-clad fiber.

Several experiments were performed in which the output power level of the sensor was first observed when the fiber system was in air, and then when it was immersed in water. The only difference in power level was caused by bending loss.

Several different lengths of aluminum-clad fiber were tested to analyze the effects of the sensing length. Different wavelengths of optical source were also used. The output power level of the aluminum-clad fiber sensor system, immersed in NaOH was monitored and plotted against time. The plots are shown in the next chapter.

6.0. EXPERIMENTAL RESULTS AND DISCUSSION

Several different experiments were performed to validate the theories proposed in Chapter 4. The three layer surface plasmon sensors were interrogated with a white light source to determine the effects of different refractive indices with both the single mode and multimode configuration. The aluminum-clad fiber sensor was etched in a bath of NaOH to simulate the process of corrosion.

6.1 Experimental Results and Discussion of the Kretschmann Prism Experiment

A simple experiment was performed to verify the SPR principle using the Kretschmann prism arrangement. The output intensity of light at different incidence angles for a specific sample refractive index were observed. Figure 6.1 shows a plot of the output intensity of light with respect to the angle of minimum detection for specific refractive indices of sample solutions. As predicted, the angle of minimum detection moves with the introduction of solutions with different refractive indices.

6.2 Experimental Results and Discussion of the Three Layer SPR Experiments

Three different optical fibers were used in the generation of surface plasmon resonance using the three layer configuration. As described in Chapter 4, the fiber sensors were constructed by coating the sensing section with a layer of 44 nm of silver. In performing the experiments, a spectrum was captured of the response of the SPR fiber sensor in air without the introduction of any solution; this output wave form was chosen as the baseline. Upon the introduction of sample refractive indices, the output response of the sensor was saved and the results shown are the difference between the output response of

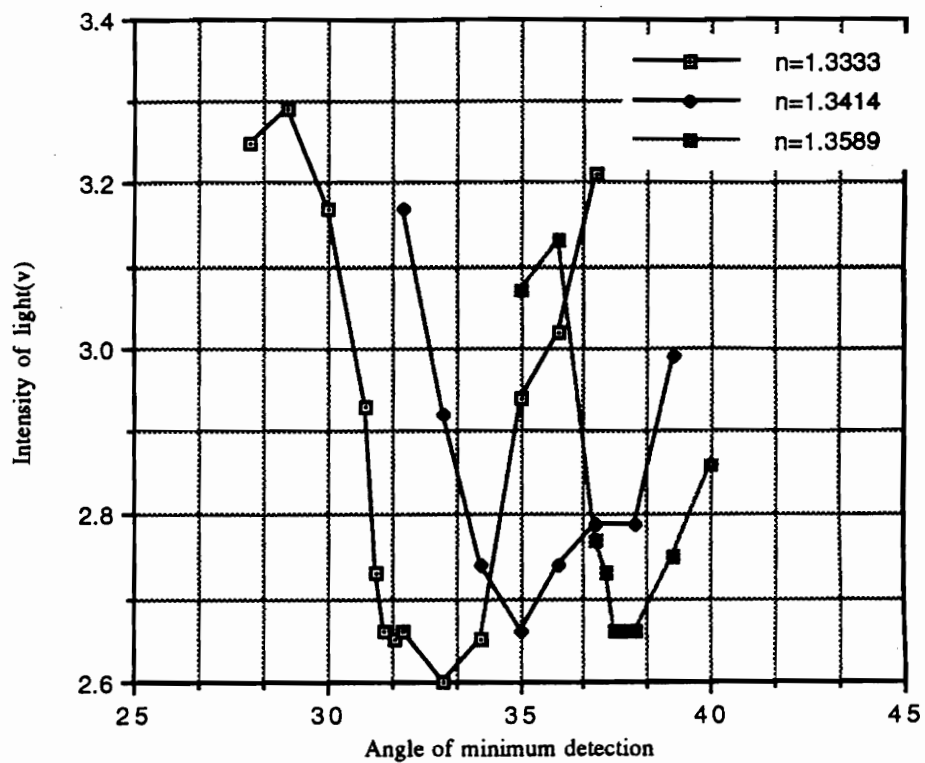


Figure 6.1 SPR test on Kretschmann prism arrangement.

the sensor with the sample solution and the baseline response. This allowed us to gain an idea of the effects of the different refractive indices.

6.1.1 The single mode fiber sensors

The single mode SPR sensors were interrogated with the white light source and the results were more noisy than expected. Figure 6.2 shows a sample of a wave form with a sample refractive index of $n=1.4142$. The approximated resonance wavelength is 579 nm. But as can be seen, The response of the sensor to white light is very noisy and not accurate. The white light source did not output a lot of power and hence the results were noisy and clear peaks were not observed. With the approximated resonance wavelengths observed from other similar output wave forms from the OSA, Figure 6.3 shows a plot of the experimental data. As expected, the resonance wavelengths moved as different sample refractive indices were introduced. This proves that the sensor is capable of responding to various refractive indices. The resonance wavelengths shifted from 525 nm to 778 nm for a Δn of 0.073 showing a responsivity of 2.885×10^{-4} refractive index units per nanometer.

6.2.2 Polished multimode fiber sensors

The polished multimode fiber sensors were interrogated with a white light source in the same method as that for the single mode polished sensor. There was a tremendous increase in throughput power (approximately 25 dB). With this increase in throughput power, the wave forms looked less noisy and an approximated resonance wavelength was more easily deduced. Figure 6.4 (a) shows the response of the sensor to $n=1.333$ while Figure 6.4 (a) shows the response for a sensor to a refractive index of $n= 1.4172$. The resonance wavelength moved from 520 nm to 725 nm for Δn of 0.0842. Thus, the

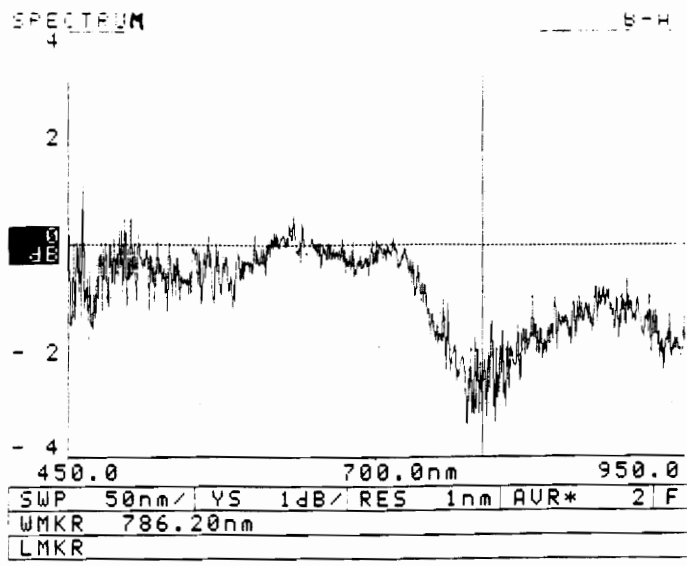


Figure 6.2 Sample waveform of a single mode polished fiber SPR sensor with a sample refractive index = 1.4142.

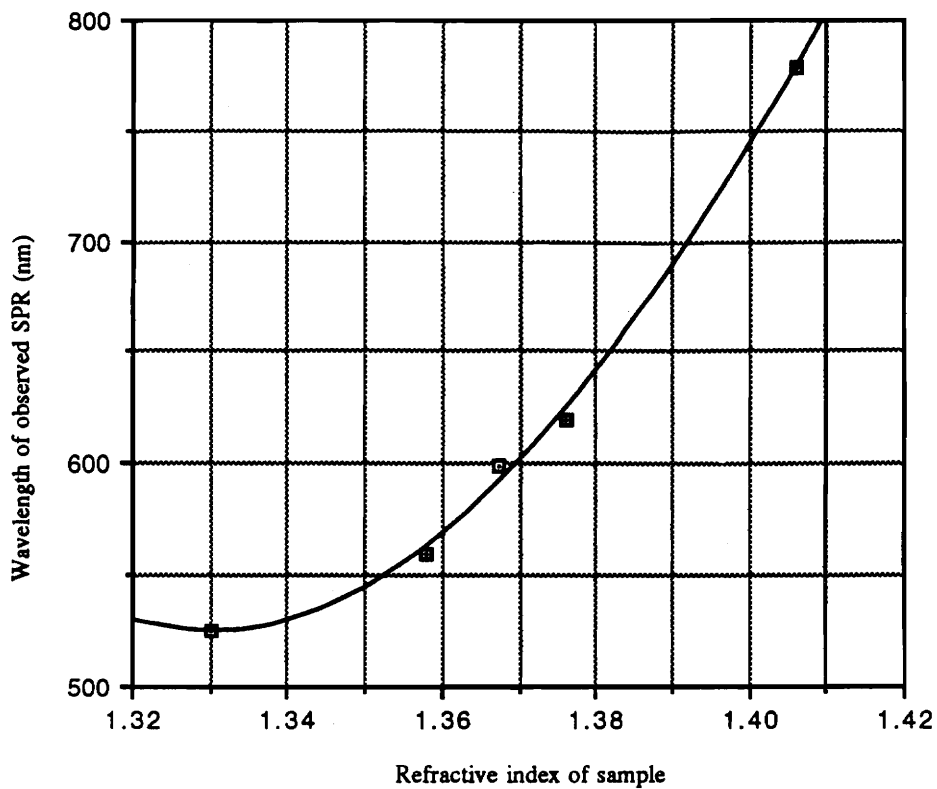


Figure 6.3 Wavelength of observed surface plasmon resonance for different sample indices using the single mode fiber sensor.

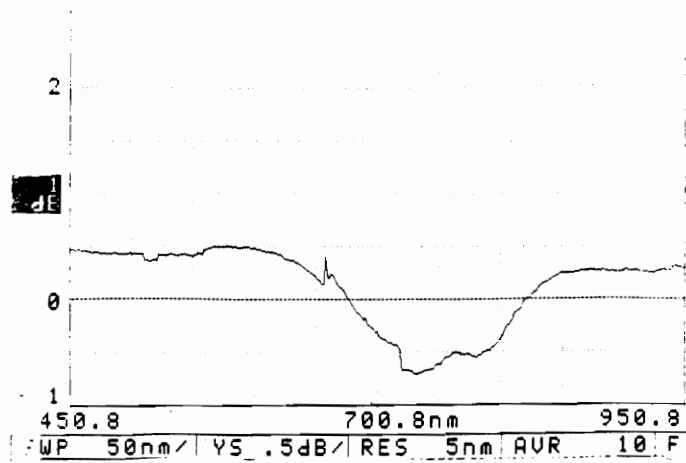


Figure 6.4(a) Sample waveform of a multimode fiber based SPR sensor with a sample refractive index = $1/333$

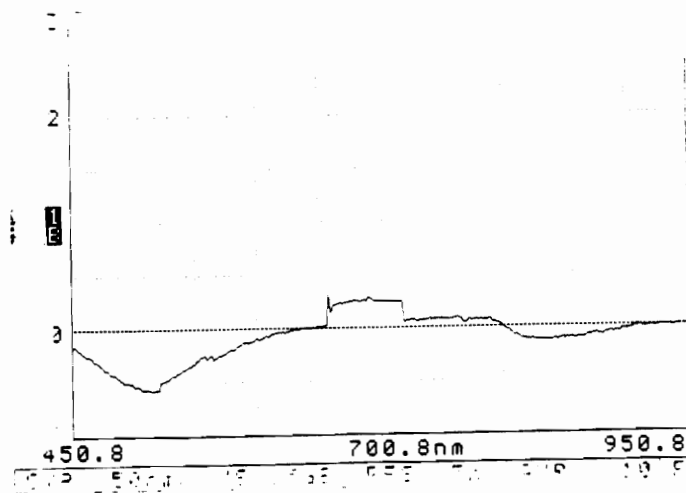


Figure 6.4(b) Sample waveform of a multimode fiber based SPR sensor with a sample refractive index = 1.4172 .

responsivity of the sensor is about 4.1073×10^{-4} refractive index units per nm. Figure 6.5 shows the resonance wavelengths versus sample refractive indices.

6.2.3 Multimode unpolished fiber sensors

The multimode unpolished sensors were interrogated with a white light source and also showed a good response with the increased throughput power. This sensor showed the most linear shift in wavelength in response to different refractive indices. Figure 6.6(a) shows the output response of the sensor to a sample refractive index of $n=1.3595$ and Figure 6.6(b) shows the response of the sensor to a sample refractive index of $n=1.3856$. As can be seen, the refractive index has shifted with the increase in sample refractive index. This sensor's resonance wavelength moved from 540 nm to 800 nm for a Δn of 0.081 for a responsivity of 3.115×10^{-4} refractive index units per nanometer. Figure 6.7 shows the shift of resonance wavelengths with different sample refractive indices.

A simple test was performed to check the repeatability of the sensors. The multimode unpolished sensor was interrogated with the white light source and sample solution were introduced with unknown refractive indices. As shown in Figure 6.7, a curve fit was performed on the data. Using this curve fit, the refractive indices of the unknown solutions was interpolated.

$$n(\text{interpolated}) = 1.3630807 \quad n(\text{actual}) = 1.3625 \quad \Delta = 0.0005807 \quad \text{error \%} = 0.0426$$

$$n(\text{interpolated}) = 1.3916055 \quad n(\text{actual}) = 1.3860 \quad \Delta = 0.0056055 \quad \text{error \%} = 0.4044$$

The minimum detectability of the sensor = sensitivity of the sensor

$$= \text{slope of curve} \times \text{sensitivity of OSA}$$

$$= 4.0253 \times 10^{-4} \times 2 \text{ nm}$$

$$= 8.04 \times 10^{-4}$$

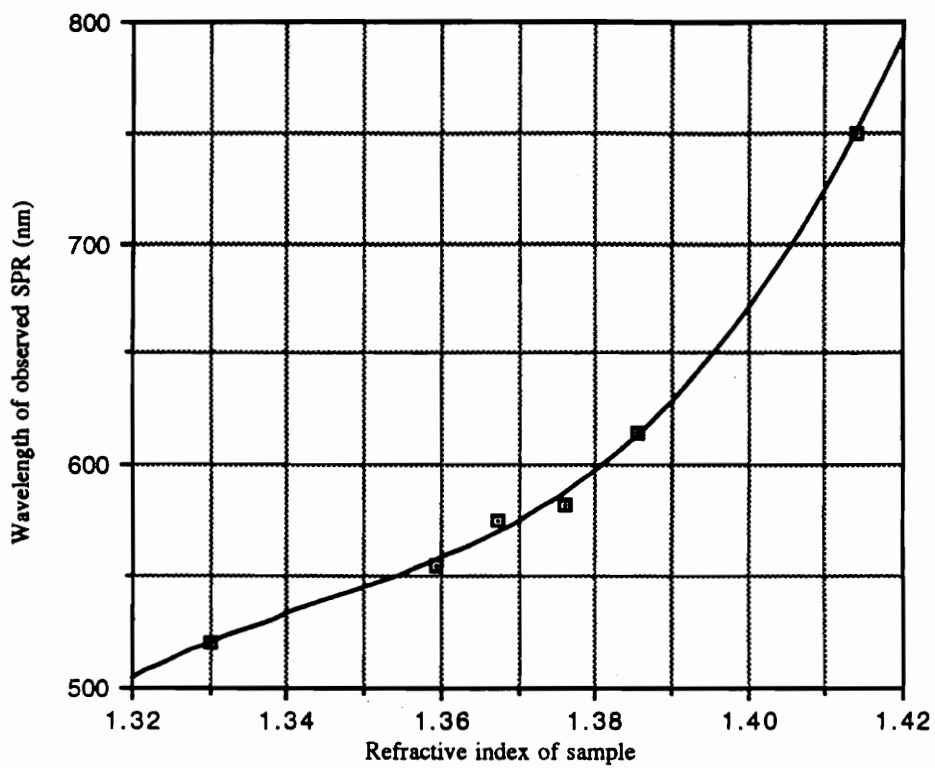


Figure 6.5 Wavelength of observed surface plasmon resonance for different sample refractive indices using the multimode polished fiber sensor.

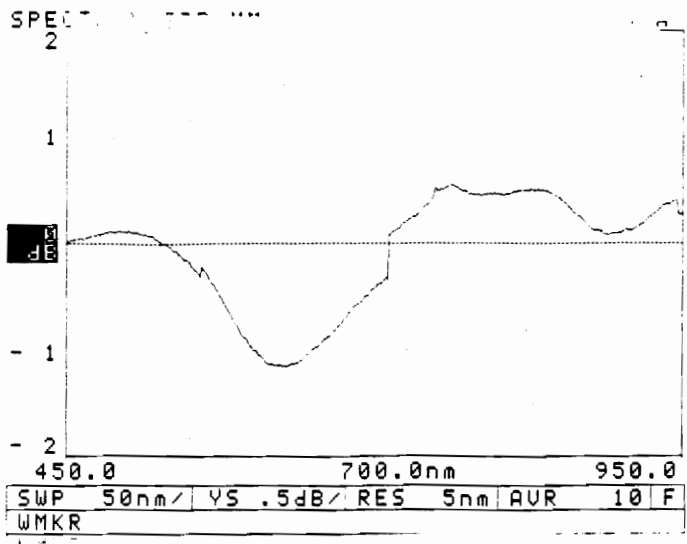


Figure 6.6(a) Sample waveform of an unpolished multimode fiber-based SPR sensor with a sample refractive index = 1.3595.

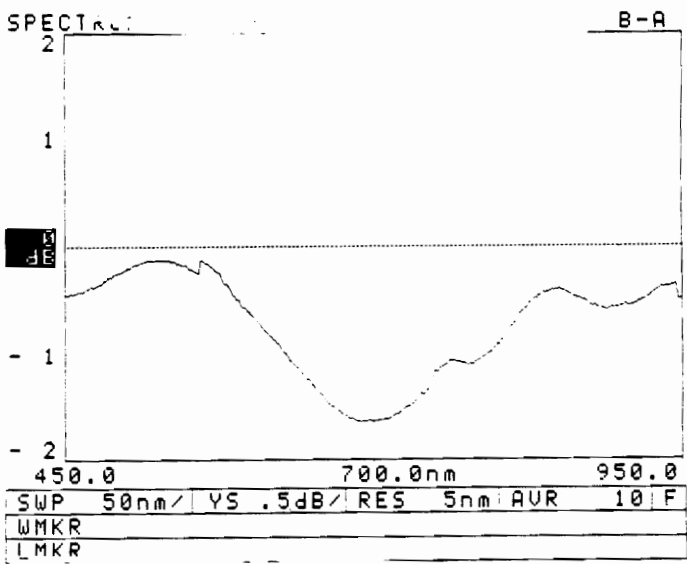


Figure 6.6(b) Sample waveform of an unpolished multimode fiber-based SPR sensor with a sample refractive index = 1.3856

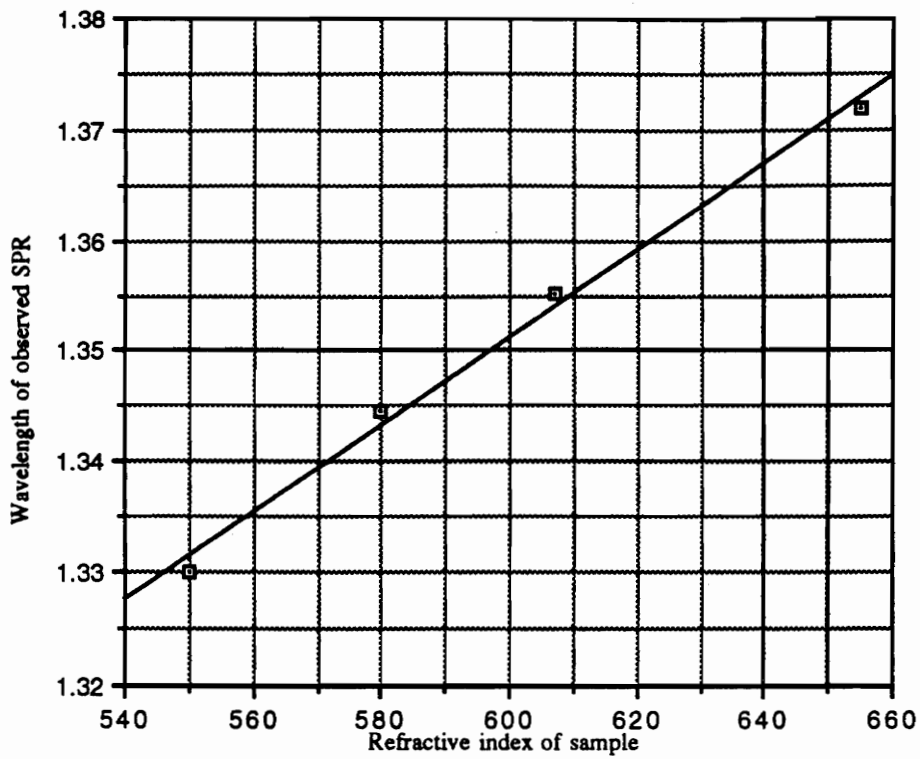


Figure 6.7 Wavelength of observed surface plasmon resonance for different sample refractive indices using the multimode unpolished fiber sensor.

Therefore, the error in the first case is less than the sensitivity of the sensor but the second is greater than the sensitivity of the sensor and is therefore an error. There are two possible reasons for this error. The first being that the solution may not be pure and secondly, there were not enough data points to provide an accurate interpolation.

6.3 Applications of the fiber-based surface plasmon sensor

The fiber-based surface plasmon sensors can be used in many varied applications. The major application of this sensor would be to detect changes in refractive indices. A dip probe configuration can be eventually attempted so that this sensor can be conveniently introduced into an unknown solution. This application would be very useful for chemical and pharmaceutical companies.

This sensor can also be used as a biochemical sensor for the clinical analysis of biochemical interactions between antibodies. If for example, one member of a biochemical pair is adsorbed onto the metal surface and the biological conjugate is introduced, the reaction between the two will increase the amount of material at the surface of the metal. This in turn will cause an increase in amount of material at the surface causing a shift in the resonance wavelength.

Corrosion monitoring can also be one of the applications of the sensor. Since the sensor is very sensitive to the thickness of the material present, as the aluminum corrodes, this will cause the resonance wavelength to shift providing a method to monitor the amount of corrosion in the environment of the sensor.

This sensor can also be used to check the purity of solutions as well as in chemical flow injection analysis in process plants.

6.4 Future Work with the Fiber-based SPR Sensors

An initial investigation of the concept of white light interrogation of the single mode and multimode SPR sensors has been attempted. It has been shown that the sensor responds to various refractive indices, causing an appreciable increase in resonance wavelengths but the research on this sensor is by no means over. A theoretical model of this sensor has been attempted but has not been completed because of the lack of time. The effective index of the fibers vary with frequency and work is being done to quantify that result at this present time. With a sound theoretical model, this research will be the beginning of a new era of fiber-based SPR sensors to monitor biochemical reactions, corrosion, etc. Work will also be done in considering this sensor for a dip probe application as a convenient versatile sensor. A more powerful white light source will also produce better results.

6.5 Aluminum-clad fiber sensor experimental results and discussion

The aluminum-clad fiber was tested for corrosion monitoring with many different lengths of sensors and optical sources in a bath of NaOH as described in Chapter 5. The response of the sensor was very similar as shown in Figures 6.8-6.10. The amount of time required for the sensor to fully etch in the same concentration of NaOH, depended on the length of the sensor. As would be expected, the longer the sensing length, the more time it took to etch the fiber.

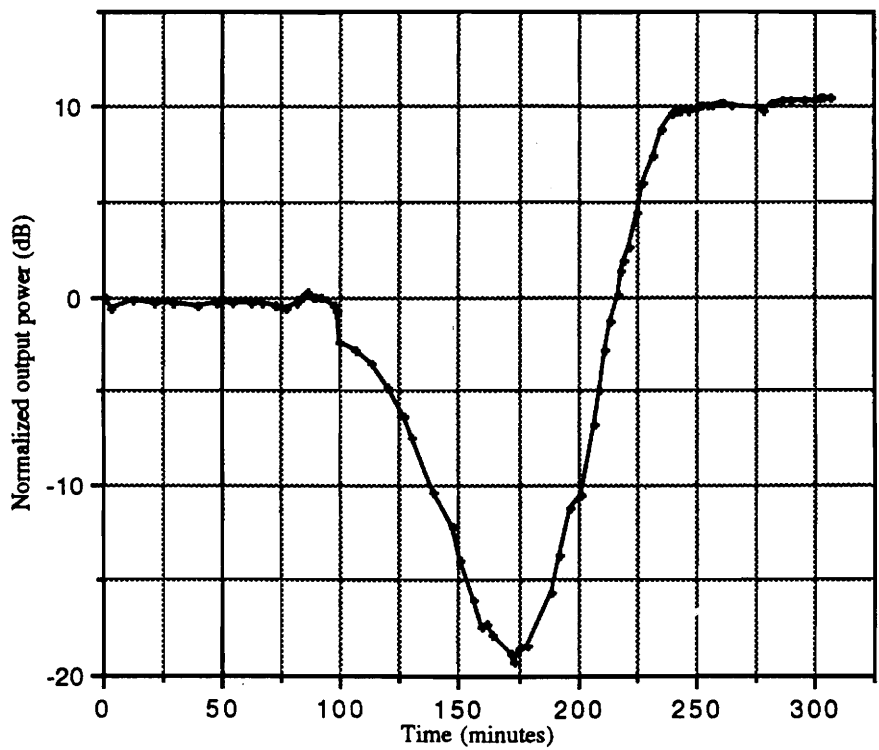


Figure 6.8. Output power vs. time aluminum-clad fiber test using a 1300 nm optical source.

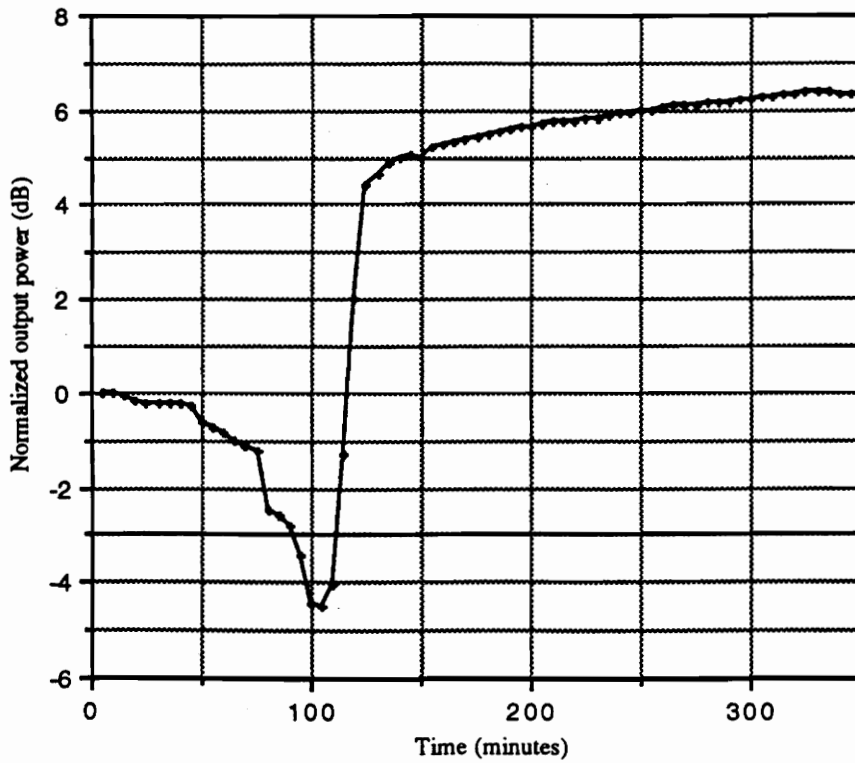


Figure 6.9 Output power vs. time for an aluminum-clad fiber etch using an 850 nm optical wavelength LED.

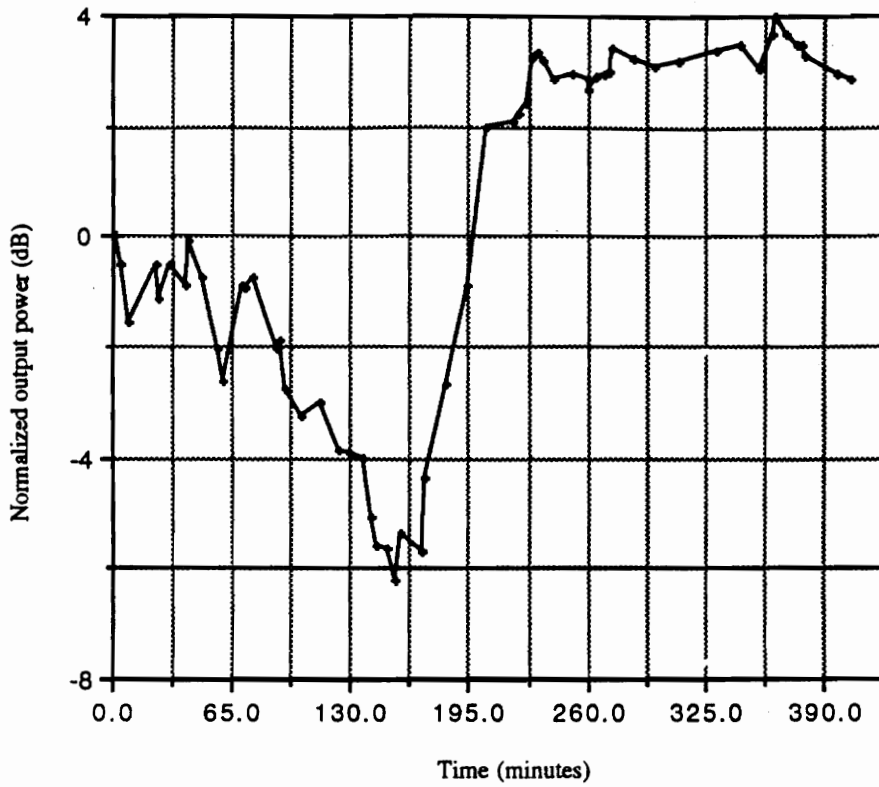


Figure 6.10. Output power vs. time for an aluminum-clad fiber etch test using a 633 nm optical source.

It was observed that all the sensors showed the same behavior to the NaOH. When the test began, the power level initially remained relatively constant because the refractive index of the aluminum is very high (~ 7-12 depending on the wavelength), much higher than that of silica glass. The refractive index of the core must be higher than that of the cladding to cause total internal reflection and confinement of light in the core. In this scenario, there is no total internal reflection along the sensing length, only reflections out of the core causing most of the light to escape out of the core. Thus, the initial output power level is very low. As the aluminum continues to etch, we continue to observe no change in the sensor output till the evanescent region of the fiber is approached. There is a sudden drop in power observed at this time because of the presence of surface plasmons. The scenario present is perfect for the formation of surface plasmons. A small layer of a suitable metal is present with the presence of NaOH as the sample with a refractive index of 1.413 nm. The surface plasmon resonance causes the attenuation of light and this attenuation is present till all the aluminum is totally etched. There is a finite period of time while all the aluminum is etched because all the aluminum will not be removed around the fiber at the same time. This explains the presence of the gradual increase in power. As all the aluminum is etched, the power level reaches a steady level because now the core effectively has NaOH as the cladding, which having a lower refractive index than the core causes propagation of light along the sensor.

The reason that the magnitude of the dip is different for the various optical sources is because of the phenomenon of mode field diameter of the fiber. As the wavelength of the source increases, the evanescent region of the core penetrated further into the cladding. Hence, for the 1300 nm laser, the area for the surface plasmon resonance to penetrate is

larger and thus, the attenuation persists for a longer period of time causing it to have a larger magnitude.

6.6 Applications of the aluminum-clad fiber sensor

Thus, it can be seen that a sensor has been fabricated that has the capability to monitor corrosion. If water or moisture were to be present in the atmosphere of the sensor, the aluminum would gradually corrode with time. If the sensor was monitored regularly, the level of corrosion of the neighborhood of the sensor can be gauged. If this sensor is required to be attached to a mobile unit such as an airplane, the sensor can be conveniently manufactured to be able to connect to a source and detector to be monitored at regular intervals.

6.7 Future Work with aluminum-clad fiber sensors

The aluminum-clad fiber sensor has shown to produce a response to corrosion that is reproducible with any source of light and sensing length. Future work will begin in attempting a tapered fiber configuration. If a tapered fiber is used, a section of the fiber that has less aluminum will etch away quicker, causing an early increase in power. In the configuration used now, there is a drastic increase in power when all the aluminum etches. Since the whole sensing length has the same thickness of aluminum, all the aluminum etches at relatively the same time. If a linearly tapered fiber is fabricated, there will be an increase in power early in the process and the power will increase linearly with time till all the aluminum is etched. Figure 6.11 shows the comparison between equal length sensors that were both interrogated with a 1300 nm laser. One of the sensors is a regular sensor while the other sensor has a 4-level taper. A 4-layer taper implies that there are four varying thicknesses of aluminum from 20 μm to 5 μm . A linear taper cannot be fabricated

at this time because of the lack of a proper tapering stage. As can be seen, there is a longer period of time when there is a linear increase in power in the 4-level taper. Thus, work has begun in this direction but a linear taper is the ideal solution to this problem

This sensor is also very fragile and breaks easily. Research should be attempted to fabricate a stronger and more durable sensor. More research is also required in understanding the processes at work during corrosion of the aluminum of the sensor and the surface plasmon resonance produced.

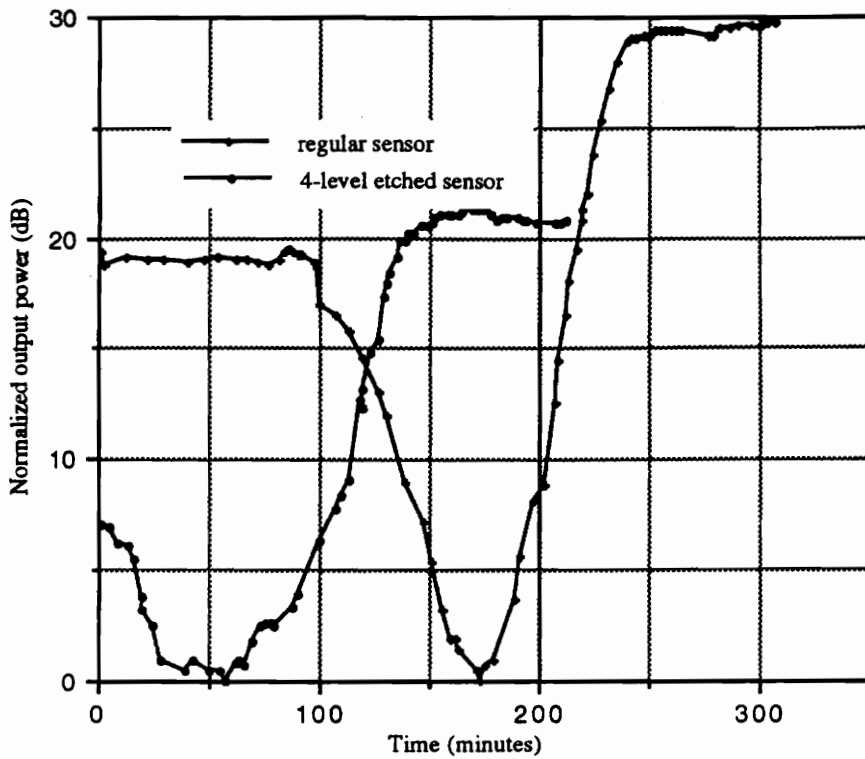


Figure 6.11 Comparison of the output power vs. time for two 10" aluminum-clad fiber sensors using 1300 nm optical sources; a regular sensor and 4-level etched sensor.

7.0 CONCLUSIONS

The objective of this research is to perform chemical sensing using fiber optics. One of the major objectives was to monitor metallic corrosion because corrosion is a serious problem in all metallic structures. A sensing system that can monitor metallic structures continuously for corrosion is more cost-effective than the conventional methods in which the corroding metallic structure is dismantled periodically and checked for corrosion. Such a method of continuous monitoring would eventually produce safer metallic structures as well as a more efficient and economic way to monitor corrosion. The corrosion of aluminum was chosen as the focus of this research. Another focus of this research is the implementation of a fiber optic sensor to measure refractive indices of unknown solutions.

The sensor system described here is based on two concepts. The first is a type of intrinsic fiber sensor which functions by coupling optical energy propagating in the fiber to a surface plasmon on a metallic film which has been deposited onto the surface of the fiber. The coupling of energy between the core and plasmon is very strongly dependent on the refractive index of the chemical sample which translates to an attenuation at a certain wavelength of light.⁷ The sensors tested here were injected with a white light source which results in the observation of attenuations at different wavelengths as seen on the white light spectroscope. The interrogation of the sensor with white light produces a general purpose sensor that is capable of sensing a wide variety of refractive indices. This sensor has been shown to respond with reasonable accuracy with the three configurations of polished single mode, polished multimode and unpolished multimode sensors. If a more powerful white light source could be utilized, the single mode sensor would prove to be a

very useful sensor as it will provide a very narrow response to the sample refractive index. This response of the sensor has been proven to shift with varying refractive indices of sample solutions. Work is required in deriving a theoretical model for this sensor.

The second type of sensor is a transmissive aluminum-clad fiber sensor where the core of a standard fiber is coated with 40 micrometers of aluminum. Varying lengths of aluminum-clad fiber are mechanically spliced to standard multimode fiber of 140/180 micrometers core and cladding diameter. As the aluminum is removed, the transmitted power level will increase. The main use of this sensor is to monitor aluminum corrosion. This sensor showed an appreciable increase in power as all the aluminum was removed. A 4-level tapered sensor was also attempted in moving toward a linearly tapered transmissive aluminum-clad fiber sensor that will provide a linear response to corrosion.

REFERENCES

1. R. O. Claus, "Fiber Optic Sensor-Based Smart Materials and Structures", IOP Publishing Ltd., 1092, Philadelphia.
2. Z. G. Wang, "Simultaneous Measurement of Strain and Temperature using two-mode elliptical core optical fiber", Thesis.
3. A. Wang, S. Gollapudi, R. G. May, K. A. Murphy, and R. O. Claus, *Optics Letters*, 16, pp. 1544, 1991.
4. K. A. Murphy, M. F. Gunther, A. M. Vengsarkar, and R. O. Claus, *Optics Letters*, 16, pp. 273, 1991.
5. B. D. Zimmermann, R. O. Claus, D. A. Kapp, and K. A. Murphy, *J. Lightwave Tech.*, 8, pp. 1273, 1990.
6. M. F. Gunther, A. Wang, B. R. Fogg, S. E. Starr, K. A. Murphy, and R. O. Claus, Presented Paper, Proceedings of the Conference of the S.P.I.E., Boston, MA 1992.
7. W. J. H. Bender, "A Chemical Sensor Based on Surface Plasmon Resonance on Surface Modified Optical Fibers", Dissertation.
8. J. M. West, "Basic Corrosion and Oxidation", Ellis Horwood Ltd., West Sussex, England, 1986.
9. D. Slutzkin, "Theory of Corrosion", Keter Publishing House Jerusalem Ltd., Jerusalem, Israel, 1976.
10. "Handbook for Structural Engineering Repairs", Vol. 1, Chp. 11, produced by the Aviation Depot, North Island, San Diego, California.
11. "Corrosion Prevention and Control", by Boeing Commercial Sirplanes, Seattle, Washington, 1988.
12. G. C. Moran, and P. Labine, "Corrosion Monitoring in Industrial Plants", ASTM 1986.
13. "Aircraft Corrosion", AGARD conference proceedings, No. 315, April 1981.
14. A. R. Bond, "Corrosion Detection and Evaluation by NDT", *British Journal of NDT*, Vol. 17, N0. 2, pp. 46-52, 1971.

15. J. P. Watjen, and A. J. Bahir, "Evaluation of a novel eddy current probe for detecting cracks inside and at the edge of holes", *Electronics Lett.*, Vol 15, 1989.
16. A. Otto, "Excitation of Non-radiative Surface Plasma Waves in Silver by the Method of Frustrated Total reflection", *Z. Physics*, 216, pp. 389, 1968.
17. H. Raether, " Surface Plasma Oscillations and their Applications", in *Physics of Thin Films*, 9, Academic Press, New York, 1977.
18. W. M. Robertson and E. Fullerton, *J. Opt. Soc. Am.*, 6, pp.1584, 1989, .
19. S. Hyashi, T. Yamada, and H. Kanamori, *Optics Comm.*, 36, pp. 195, 1981.
20. W. H. Weber, and S. L. McCarthy, *Physical Review B*, 12, pp. 5643, 1975.
21. Y. Mao, H. A. Macleod, and K. Balasubramanian, *Applied Optics*, 28, pp. 2914, 1989.
22. B. Liedberg, C. Nylander, and I. Lundstrom, *Sens. Act.* , 4, pp. 299, 1983.
23. R. P. H. Kooyman, H. Kolkman, J. Van Gent, and J. Greve, *Anal. Chem. Acta.*, 213, pp. 35, 1988.
24. P. B. Daniels, J. K. Deacon, M. J. Eddowes, and D. G. Pedley, *Sens. Act.*, 15, pp. 11, 1988.
25. I. Pockrand, *Surf. Sci.*, 72, pp. 577, 1978.
26. D. Y. Song, F. S. Zhang, H. A. Macleod, and M. R. Jacobson, SPIE, 678, Optical Thin Films II: New Developments, pp. 211, 1986.
27. Pharmacia Biosensor AB, S-751 82 Uppsala, Sweden.
28. W. Johnstone, G. Stewart, T. Hart and B. Culshaw, "Surface Polaritons in Thin Metal Films and their Role in Fiber Optic Polarizing Devices", *J. Lightwave Tech.*, Vol. 8, No. 4, pp. 538, April 1990.
29. M. N. Zervas, " ", *IEEE Photonics Letters*, 2, pp. 253, 1990.
30. R. C. Jorgenson, S. S. Yee, S. Johnston, and B. J. Compton, "A Novel Surface Plasmon Resonance Based Fiber Optic Sensor Applied to Biochemical Sensing", SPIE, Vol. 1886, pp.35, 1993.

31. H. E. de Bruijn, R. P. H. Kooyman and J. Greve, "Choice of Metal and Wavelength for Surface-plasmon Resonance Sensors: Some Considerations", *Applied Optics*, Vol. 31, No. 4, pp. 440, February 1992.
32. W. J. H. Bender, R. E. Dessy, M. S. Miller, and R. O. Claus, " The Development of a Chemical Sensor Based on Surface Palsmon Resonance on Surface Modified Optical Fibers".

VITA

Anjana Nagarajan was born in Kottayam, India on March 4, 1970. daughter of Alamelu and S. Nagarajan. She moved to Bangalore in 1977 and graduated from Baldwin Girls' High School in May 1988. She received her BS. in Electrical Engineering from the Bradley Department of Electrical Engineering at Virginia Tech in May 1992. She started her graduate studies at FEORC under Dr. Claus immediately after. This thesis is a result of the work at FEORC. After graduation, she plans to work as a Technical Leadership Development Program Engineer with Ericsson-GE Mobile Communications in Lynchburg, Virginia.

Anjana